THE UNIVERSITY OF ALBERTA

INTERACTION OF STRAIN-CYCLING AND DIFFUSION IN COPPER-BRASS COUPLES

by

THIRUMALESHWARA BHAT A.

A THESIS

SUBMITTED TO THE FACULTY OF GRADUATE STUDIES

IN PARTIAL FULFILMENT OF THE REQUIREMENTS FOR THE DEGREE

OF MASTER OF SCIENCE

IN METALLURGICAL ENGINEERING

DEPARTMENT OF MINING AND METALLURGY

EDMONTON, ALBERTA

February, 1968

UNIVERSITY OF ALBERTA

FACULTY OF GRADUATE STUDIES

The undersigned certify that they have read, and recommend to the Faculty of Graduate Studies for acceptance, a thesis entitled

INTERACTION OF STRAIN CYCLING AND DIFFUSION
IN COPPER-BRASS COUPLES

submitted by THIRUMALESHWARA BHAT A.

in partial fulfilment of the requirements for the degree of Master of Science.

ACKNOWLEDGEMENTS

The author expresses his sincere gratitude to Dr. F. H. Vitovec for his unfailing guidance and supervision during the course of this project and its writing. He is indebted to Professor E. O. Lilge, under whose departmental supervision the project was completed. He is grateful to Professor D. G. W. Smith of the Department of Geology for his help in the electron-microprobe analysis.

The help received from the technicians of the department, Mr. Scott, Mr. Fitzgerald and Mr. Forman, is very much appreciated.

The author is gratefully indebted to the National Research Council of Canada for their financial assistance.

TABLE OF CONTENTS

LIST OF FIGURES

LIST OF FIGURES (continued)

1. INTRODUCTION

Interest in the effect of strain on diffusion has been stimulated by the recognition of the role of crystal lattice imperfections such as vacancies, interstitials and dislocations in solid state diffusion. The types of strain or stress that may affect diffusion are:

1. elastic strain during diffusion,
2. plastic strain during diffusion, and
3. plastic deformation of the metal prior to diffusion.

It is convenient to consider elastic and plastic deformations separately. In the case of elastic deformation, one has to note that compression or expansion of the lattice will alter the ease of atom movements. Its effect on the thermodynamic driving force for diffusion was studied by Konobeevski et al. (1). Experiments on the pressure dependence of the diffusivity, D, showed that the diffusivity is reduced by a hydrostatic pressure in an exponential manner (2,3,4,5,6,7). For example, a pressure of 30 kilobars reduced the diffusivity of lead in the temperature range 250° - 300°C by three orders of magnitude (7). The effect of pressure is expressed by a change in the activation energy by an amount proportional to the pressure.

$$\text{Thus, } D_p = D_o \exp\left[\frac{-(Q + \alpha p)}{kT}\right]$$

where D_p is the diffusivity under pressure,

and α is a positive quantity, called "activation volume." Although the above consideration is rather simple, the case of an

arbitrarily stressed body (including gradients of stress) is complicated because of lack of a quasi-equilibrium state of shear stress during a general diffusion process. However, restricted cases such as relaxation were analyzed (8).

The effects of lattice distortions accompanying the formation of a solid solution have been also subjects of study (9,10,11). Some authors reported an influence of thermal stresses on diffusion (12,13). Pronounced enhancement of diffusion by irradiation is also reported (14).

Plastic deformation prior to diffusion anneal may cause enhancement of diffusion by an increase of the lattice imperfections. The direct effect of cold-working was studied by Andreeva (15).

Plastic deformation during diffusion may enhance diffusion basically in two ways:

1. by an increase of the vacancy concentration,
2. by an increase of the dislocation density.

Let us first consider the effect on the vacancy mechanism. The activation energy "Q" for diffusion by the vacancy mechanism is the sum of the energy of formation of a vacancy E_f and that of migration E_m. The quantity exp $-(E_f/kT)$ in the expression for the diffusion coefficient is proportional to C_v, the concentration of vacancies. Plastic strain leads to the production of vacancies in excess of the number present in thermodynamic equilibrium. If, then, these vacancies are not destroyed again too quickly and if there is a continuous supply of these excess vacancies, diffusion can be expected to be enhanced. To provide this state, the specimen must be strained continuously throughout the diffusion anneal.

Let us now consider the dislocation mechanism. Diffusion along dislocations occurs at a higher rate because of the more open structure of

the crystal lattice along the core of the dislocation. This is sometimes called "diffusion short circuiting" or "pipe diffusion." Thus the overall diffusivity will depend on the dislocation density of the metal. Then, any process which would increase the dislocation density, such as plastic deformation, should enhance the diffusivity.

Reports on the effect of plastic deformation on diffusion date back to 1921, but it was only in 1952 that a first systematic study was done by Buffington and Cohen (16). Data from several investigations, which were published later, are listed in Table 1 (17). The results vary in a wide range from no enhancement at all to significant enhancements. While it is evident that plastic deformation may produce observable effects on the rate of diffusion, particularly at low temperatures, there still are doubts regarding the magnitude of the effect and the range of temperature for which it is significant. Thus it is impossible on the basis of the available information to specify whether the strain-enhanced diffusion, if at all true, is a result of the generation of mobile point-defects by moving dislocations or if it is mainly due to dislocations and sub-boundaries.

Brown and Blackburn are of the opinion that in those experiments where enhancement was observed, the calculated values of depths of penetration ($2\sqrt{D_e t}$) were too small for accurate measurement of the diffusivity D; and that, where no enhancement was found, the values of the depths of penetration ($2\sqrt{D_e t}$) were adequate (17). (D_e is the theoretical diffusivity in an unstrained system.)

Duhl, Taranto and Cohen argued that, at least in the case of the residual-activity technique of analysis, the observed enhancements due to plastic flow could not be explained away by the existence of small penetration distances (26). They supported their view by observations on gold with $2\sqrt{D_e t}$ values of 2 to 50μ, where enhancement by a factor of 10 was observed. The same authors also quote a reported increase of diffusion rate in α-iron

under compressive plastic flow, as analyzed by the residual-activity technique.

Killpatrick and Balluffi also observed enhancement, but explained it by the cracks, which formed during straining.

From the above information it is not possible to come to any definite conclusion.

In order to produce enhancements by strain, the number of excess atomic jumps must be significant compared to the number of atomic jumps occurring in the lattice under ordinary conditions. According to Ruoff and Balluffi (27,28,29), the rate of excess point-defect production and the life-time of these vacancies are sufficiently small during the high-temperature deformation of typical metals so that any deviation from the usual equilibrium vacancy concentration should be below the limit of detection in the usual diffusion experiments. Under certain conditions the observed bulk-diffusivity may be markedly enhanced by fast diffusion-short-circuiting along static or moving dislocations or along cracks. Large apparent enhancements may be erroneously derived from experiments, when uncorrected effects due to specimen distortion cause the experimentally determined diffusion penetration curve to appear falsely wide. Based on the analysis of a large set of experimental results Ruoff and Balluffi (29) conclude that at temperatures greater than about half the absolute melting point no macroscopic enhancements of diffusion have been observed. Two reported enhancements (30) are attributed to possible short-circuiting. Two other reported enhancements are attributed to experimental difficulties with specimen distortion.

It has been shown that impractically high strain rates are required to produce a sufficiently high excess of lattice imperfections for

observable enhancement of diffusivity. A large increase in the diffusivity is theoretically possible due to dislocation-short-circuiting, especially at low temperatures. However, even at temperatures as low as 1/3 of the absolute melting point, the increase may be still too small to be detected by usual techniques for practical diffusion times (31).

Information on enhancement of diffusion may be obtained indirectly from certain other diffusion-controlled phenomena. Shepard and Sherby (32) suggest that creep characteristics like strain-softening, time-dependent strain rates and breakdown of the power-law for the stress-sensitivity of the creep rate at high stresses can be explained by an enhanced atomic mobility due to plastic straining. The authors believe that these creep characteristics are due to the creation of excess lattice vacancies by the motion of jogged screw dislocations during plastic deformation. Short-circuiting by dislocations in subgrain boundary plays a major role in enhancing diffusion, but dislocations in other configurations appear to be unimportant.

Observations of fatigue properties may also indicate the occurrence of enhancement. According to Forsyth, precipitates grow in persistent slip bands during fatigue in age-hardened alloys (33). Broom et al. (34) point out that an alloy like DTD 683, which derives its static strength from unstable precipitates, shows poor fatigue properties due to overaging of the precipitates under reversed strain caused by fatigue stress. However, Laird and Thomas (35) recently remarked that the low fatigue strength is due to already existing precipitate-free bands and not due particularly to over-aging of precipitates.

Enhancement by ultrasonic irradiation has been reported by two different groups of investigators (36,37). The authors observed that the

enhancement is proportional to the intensity and independent of the frequency of the ultrasonic vibrations.

The above review shows that:

1. the topic of enhancement of substitutional diffusion is still subject to controversy, and
2. enhancement is expected to be more pronounced at lower temperatures, at which not only the mean life of vacancies is longer, but also grain-boundary diffusion is predominant.

The above points need to be observed in establishing a test program. In order to produce observable enhancement tests should be carried out at low temperatures, where grain-boundary diffusion is predominant. The form of straining may have a bearing on the degree of enhancement.

Unidirectional straining has the shortcoming that at high strain rates at which a sufficient number of imperfections are produced, strain becomes exhausted before sufficient penetration is obtained. At lower strain rates, it is possible to have sufficient time for significant penetration, but due to recovery and annealing effects the supply of excess defects may be too small to affect diffusion significantly.

Fatigue strain cycling has the advantage that the total accumulated strain can be greater than in unidirectional straining. In addition, it is possible to have higher strain rates than in unidirectional straining. Moreover, no investigations have been done previously with strain cycling at conventional frequencies.

In addition to the above advantages, strain cycling may also furnish information on the fatigue mechanisms.

It has been suggested that large numbers of vacancies are generated

during fatigue by moving dislocations with jogs (38). An enhancement of observed diffusivity by strain cycling would support this opinion.

It has been suggested that fatigue cracks are nucleated by vacancy clustering (38,39). Crack nuclei may grow by collecting vacancies in regions of bad fit in grain boundaries (40,41). Attempts to observe vacancy clusters directly has given contradictory results (42,43,44,45,46). However, the fact that metals suffer fatigue failure down to 1.7°K, where all vacancy diffusion is suppressed, raises doubt about the validity of the cluster model (47,48). The observations, that both the time for crack initiation and for propagation decrease with increasing temperature (47,48), support the view that vacancy diffusion may play some role in the fatigue mechanism. Suppose that the fatigue tests are carried out with a diffusion couple such as copper-α-brass. Vacancies are accumulated in the diffusion zone in α-brass due to nonuniform diffusion of zinc and copper. Then these vacancies could enhance fatigue damage in that region of the α-brass, if the vacancies have any role to play in fatigue damage. On the other hand, excess vacancies, generated by strain cycling in the copper and normally available for fatigue-void nucleation by the clustering mechanism, may be reduced by diffusing zinc atoms. Thus, in the diffusion zone in copper, fatigue damage may be slowed down. In addition, diffusion may be enhanced.

From recent studies on fatigue, it is evident that at temperatures above 400°C fatigue damage occurs at grain boundaries in copper and brass (49,50,51). High-temperature fatigue is characterized by dispersed fine slip within the grain and "permanent strain" due to incompletely reversible slip accumulated at grain boundaries (49). Grain-boundary diffusion affects the observed overall diffusivity in the Cu-Zn system at temperatures below about 575°C. Thus in this temperature range overall diffusivity may be

enhanced by enhanced grain-boundary diffusion. At temperatures below 400°C, fatigue damage occurs within the grains. Then overall diffusivity at temperatures below 400°C may be enhanced by enhanced volume diffusion due to the fatigue damage in the grains.

Thus fatigue strain cycling is a particularly attractive form of straining to choose because it can throw light not only on its effect on diffusion rate, but also on the mechanisms of fatigue damage at high temperatures.

2. EXPERIMENTAL DETAILS

2.1 EXPERIMENTAL PROGRAM

Diffusion experiments with and without superimposed strain cycling were carried out.

The experimental program has been designed to provide optimum conditions for the interaction of diffusion and strain cycling.

A copper-zinc diffusion system provided by an α-brass-copper diffusion couple was selected because extensive data from static diffusion experiments are available from the literature for comparison. Another advantage is the color change of the diffusion zone, which facilitates the study of the diffusion zone.

Strain cycling fatigue tests were to be conducted on composite test specimens in a range of temperature from 500°C to 700°C, extending from the temperature range, where grain-boundary diffusion is dominant to that where bulk diffusion is the controlling factor. Furthermore, in this same temperature range grain-boundary cavity formation by fatigue stressing has been reported to occur in both materials of the diffusion couple, thus indicating the possibility of the interaction of the grain-boundary mechanisms.

The method of strain cycling must be selected with consideration of the composite test-specimen configuration. The strain cycling must occur in such a manner as to provide:

1. a homogeneous strain along the entire area of the diffusion interface,
2. a uniform temperature over the entire test section,

3. mechanical stability and retention of the specimen configuration throughout the test,
4. control of the environment to prevent oxidation and other reactions,
5. compensation of creep in the specimen grips and the possibility of retightening at the test temperature without affecting the environment.

These considerations led to the selection of alternating torsion as the mode of straining.

The test specimen should have a configuration to provide a controlled and uncontaminated source of zinc. This is achieved by a cylindrical composite specimen, which consists of a core of α-brass and a surrounding cylindrical shell of copper. Even though a variable gap between the brass and copper may develop during the test a steady condition of a zinc vapor-solid copper diffusion system is maintained.

The effects of strain cycling on diffusion as well as those of diffusion on fatigue were delineated by comparison with specimens which were diffusion-annealed without strain cycling.

2.2 EXPERIMENTAL PROCEDURE

2.2.1 Test Materials and Specimen Preparation

The diffusion couples were made of OFHC copper supplied by AMAX*

---

* Copper and its chemical analysis supplied by courtesy of American Metal Climax Inc. (United States Metals Refining Division) from American Brass and Copper Company.

and a 30% zinc α-brass rod supplied locally.

The chemical composition of the OFHC copper and the brass are given in Table 2.

The specimens were made in the following manner:

Starting with a 0.5 in. diameter brass rod (as cast), the following procedure was adopted:

1. Alternate annealing and swaging to a final diameter of 0.285 in. The annealing was carried out at 300°C for one hour in a ceramic tube. Zinc was also placed in the tube on the side of argon entrance at a location of appropriate temperature to provide a zinc vapor pressure in equilibrium with α-brass and thus avoid dezincification.
2. The brass rod was then machined to a diameter of 0.253 in.

Starting with a 0.75 in. diameter rod of OFHC copper, the following procedure was adopted:

3. The copper was machined to 11/16 in. outside diameter.
4. A hole of a diameter a few thousandths of an inch less than 0.250 in. (later to be reamed to 0.250 in.) was drilled.
5. The brass and copper were annealed separately.

   Copper was annealed in an argon atmosphere at a temperature of 300°C for one hour.
6. After annealing, the copper was cleaned by chemical polishing and the inside hole reamed to a diameter of 0.250 in.
7. The brass was cleaned first by chemical polishing, followed by polishing uniformly with emery paper to a slight press-fit into the copper.
8. The couple was then swaged to 0.540 in. diameter. The swaged

couple was cut and machined into specimens of the required dimensions, the details of which are given in Figure 1.

To ensure that the brass was held in place with respect to the copper, the specimen was pinned radially with tapered steel pins in the specimen grip sections.

2.2.2. Torsion-Fatigue Testing Machine

The testing machine used for this investigation is shown in Figure 2. The main parts are the drive mechanism, the specimen and grip assembly (shown separately in Figure 3), the load cell and the split test furnace.

The 0.25 hp electric motor drives the adjustable eccentric at 750 rpm. The eccentricity can be varied from zero to 1 in., giving a range of angle of twist up to ± 8.45 degrees (Figure 4).

For assembly the flat specimen heads are inserted into the slotted grips over which long sleeves with a conical core are fitted. The sleeves are pressed over rims at the inner grip ends by nuts from the outer grip ends, thus tightening the grips. A ceramic tubing is then placed over the grip assembly. It is sealed on both ends by Viton O-rings. This assembly is fitted first into the shaft of the drive system. Then the load-cell, which slides on the frame of the testing machine, is moved to fit on the other side of the grip rod. Both grip rods are clamped to the shafts and the grips further tightened. A thermocouple is inserted through a hole in the ceramic tubing to make contact with the test specimen. A second thermocouple is placed in contact with the outside of the ceramic tubing for the control of temperature of the test furnace. Then the furnace is closed and the hoses for argon inlet and outlet are connected to the seals of the ceramic tubing. After

flushing the system with argon the assembly is ready for startup.

The heating system was calibrated using three thermocouples equally spaced over the one inch test section of the specimen. The temperature gradient over the length of the specimen was 3°C at 600°C. The furnace control held the temperature within ± 3°C.

The torque load-cell is formed by four resistance strain gauges, which are cemented on the one-inch diameter steel shaft (Figure 5). The alternating torque is monitored by a Tektronix oscilloscope using a plug-in type "Q" unit.

2.2.3. Choice of Test Temperature and Time

The temperatures were chosen, as previously mentioned, in the range 500°C to 700°C. Exploratory static diffusion experiments were conducted. Based on their results, the periods of diffusion anneal were adjusted to give sufficient diffusion penetration ($2\sqrt{Dt}$ values).

2.2.4. Choice of Strain Amplitude

First of all, fatigue tests were conducted at 600°C at various, but decreasing, strain amplitudes to find that maximum value of strain amplitude below which the life of the specimen is sufficiently long to ensure sufficient diffusion penetration.

After a number of trials it was found that the strain amplitude corresponding to a 5-degree set on the angular scale, i.e., 7.64×10^{-4} in./in. of pure shear strain at the interface, gave the desired lifetime. It may be observed that although with an increase of the temperature the fatigue life is expected to decrease, the diffusion rate increases.

For all dynamic tests the same strain amplitude was used. The strain-rate varied from zero to 6×10^{-2}/sec. The maximum value thus corresponds closely to the theoretical value of strain rate (about 10^{-2}/sec.

at a strain value of 7.64×10^{-4} in./in.) for maximum enhancement by sufficient excess vacancy production by plastic deformation (52).

All specimens were annealed at 300°C for one hour and then heated to test temperature. Strain cycling was started fifteen minutes after the test temperature was attained. Corresponding allowance was made in periods of diffusion anneal of static samples.

At the end of the diffusion anneal period, the furnace was shut off, cycling stopped and the specimen cooled by opening the furnace. The specimen attained a temperature of less than 200°C within 15 minutes. It was removed when cooled to room temperature.

2.2.5. Measurement of Diffusion Penetration

Several different methods for the measurement of the variation of concentration of the inter-diffusing metals were explored. First the conventional successive sectioning and wet chemical analysis as well as x-ray analysis were tried. Although concentration-penetration curves were obtained, this method was not pursued further because it is not sufficiently sensitive to detect small differences in diffusion rates. It does not permit consideration of the distortion of the interface or the crystallographic orientation-dependence of the diffusion rate, which results in variations of the diffusion penetration from grain to grain. In addition, this method is unable to give information about the topography of diffusion, grain-boundary penetration, etc. For these reasons x-ray microradiography and a photographic method based on color change were tried. The latter was found to be the most suitable. It was calibrated by electron microprobe measurements.

X-Ray Microradiography: The principle of the method is that secondary radiation from gallium has a wavelength, which lies between the

absorption edges of copper and zinc. The absorption edge of zinc (1.284Å) is lower than the gallium K_α radiation (1.341Å), and the absorption edge of copper (1.381Å) is higher than the gallium K_α radiation. Thus the intensity of darkening in an x-ray microradiograph of a thin section of the diffusion couple increases with zinc concentration. The x-ray microradiograph is then enlarged with transmission optical microscopy to a suitable magnification (X195) and the negative so obtained traversed on an optical microdensitometer to obtain the variation of optical density along the direction of diffusion (Figure 6).

The method was tried for several samples, but not pursued further because of difficulties associated with specimen preparation. The preparation of 40 to 50μ thick samples for microradiography was tedious and time-consuming. Moreover, the specimen showed cracks and it was difficult to avoid photographic density changes caused by non-parallel surfaces of the sample. The variation in intensity in the enlarged negative due to the grains in the x-ray film was likewise undesirable.

Photographic Method: The polished sample was photographed at a magnification of X195, using a green filter and Kodak orthochromatic metallographic plate. The particular conditions of light and the choice of plate were determined after several trials so as to produce maximum possible photographic density contrast between the red copper and the yellow diffusion zone.

The negative plate was developed in D-19 (high contrast developer) for 4½ minutes at room temperature under safelight conditions, fixed for 10-15 minutes, washed and dried.

Positive prints were made at a magnification of X2.5 with respect to the negative (total magnification X487), using Kodak Polycontrast filter

number 1 and an exposure of 10 seconds. The prints were developed in D-72 for 90 seconds, fixed, washed and dried. The paper used was Kodak Polycontrast. The conditions throughout were standardized to produce the same photographic density change at the same zinc concentration for accurate comparison.

The boundary between the white diffusion zone and the comparatively copper-rich black region on the positive print was drawn (Figure 7). Because of the standardized photographic procedure used for all samples, this line corresponds to the same concentration of zinc. This concentration was determined later by electron microprobe analysis. The area between this line and the original interface (or the area of the diffusion zone marked by color change) was then measured with a planimeter. The measurements were repeated and the average areas were determined. The average area divided by the length of the boundary along the interface on the copper side gave the average penetration distance (x) of zinc in copper.

Electron-Probe Microanalysis: An electron microprobe traverse was made on one of the specimens (Specimen number 7S) with an ARL electron-microprobe analyzer across the diffusion zone (Figure 8). Local counts were measured at the two extreme positions of the traverse (Table 3). The concentration corresponding to the point of color change in the photographic method of analysis was then evaluated from the electron microprobe traverse. Corrections for absorption and atomic number effects were applied (53) and the concentration was found to be 88.72% Cu or 11.28% Zn. The calculations are given in Appendix I.

2.2.6. Method of Calculation of the Diffusivity

Although the interface is cylindrical, it can be considered a

planar interface without appreciable loss of accuracy. By superimposing the concentration distribution curve for a planar interface over that for a cylindrical interface (54, Figure 9), it is found that for values of $Dt/a^2 < 0.01$, a diffusion across the cylindrical interface is approximately the same as that across a planar interface ("a" is the radius at the interface). In the present case, using the data in Table 4, the maximum value of Dt/a^2 obtained is given by,

$$\left(\frac{Dt}{a^2}\right)_{max} = \left(\frac{Dt}{a^2}\right) \quad \text{at } 704°C \text{ for specimen 7D}$$

$$\simeq \frac{10^{-10} \times 20 \times 3600}{\left(\frac{7}{64} \times 2.54\right)^2}$$

$$\simeq 0.932 \times 10^{-4} \ll 0.01$$

Hence the approximation.

Because of a gap between brass and copper, all the samples are essentially vapor-solid couples. The brass acts as a source of zinc vapor, which is absorbed by the copper through its surface. The high vapor-pressure component, namely zinc, diffuses more rapidly than copper and as a result the copper expands, which is known as the Kirkendall effect (Figure 10). At the same time, the Kirkendall surface becomes buried because of the smaller amount of flow of the lower vapor-pressure component, namely copper, in the opposite direction (55) (Figure 10). It has been shown by Balluffi and Seigle (55) that the concentration at the solid-vapor interface remains constant throughout the diffusion period.

Neglecting the Kirkendall effect, the diffusivity obtained will be the mutual diffusivity, D, which involves the net mass flow rather than

the individual mass flows. Since the aim of this project is not to consider the intrinsic diffusivities, but rather the effect of strain cycling on diffusion as a whole, an analysis to obtain D is sufficient. Therefore the Kirkendall effect need not be considered.

Assuming D to be independent of concentration, it can be shown that D is proportional to x^2/t, where x is the measured diffusion penetration (Figure 10) and t is the time of diffusion anneal (see Appendix II). An analysis for variable diffusivity is beyond the scope of this thesis.

3. TEST DATA AND RESULTS

The test conditions, like the testing temperature and the time of diffusion-anneal, t, are given in Table 4 together with the test results like penetration distance "x" and the measure of the diffusivity "x^2/t."

The microstructures of all static diffusion specimens showed diffusion voids in the brass (Figure 11). The nonuniformity of penetration, which is general to all samples, is illustrated in Figure 12. There were no other special features noted in the static samples.

In the dynamic samples, fatigue pores and cracks along grain boundaries were observed in some specimens, in addition to the diffusion voids in the brass (Figures 13,14,15,16). Except for specimen 7D, as can be seen from the micrographs, grain-boundary cavities became more discontinuous towards the interface.

In samples 6D, 9D and 8D, there was pronounced zinc penetration along grain boundaries with fatigue pores and sometimes even in those without such pores (Figures 17 and 18). A typical dynamic diffusion couple is shown in Figure 19. Figures 20 and 21 show the fatigue damage in the grain boundaries of copper of a dynamic sample.

The observations on the microstructure of each dynamic specimen are given in detail in the following paragraphs and a summary provided in Table 5.

Metallographic observations of the cross-section of specimen 6D showed large fatigue cracks as well as individual pores in the grain boundaries of copper, which became rather less intense towards the interface

(Figure 13). There were some visible cracks also in the diffusion zone. The penetration of zinc along these grain boundaries was remarkably high (Figure 17). In addition there was enhanced penetration along grain boundaries without visible pores. A few fatigue pores, as identified by their location along the grain boundaries, were observed in brass too (Figure 16). However, the area used for evaluation of this sample did not contain any fatigue pores or cracks.

Metallographic observation of specimen 9D revealed fatigue pores along grain boundaries in copper, with decreasing concentration from outside towards the interface. There were only one or two fatigue pores observed in the diffusion zone in the whole cross-section. It was again observed that there was greater penetration of zinc along such cracked grain boundaries. A few fatigue pores were observed in brass too. There were only one or two small pores in the area used for evaluation of the penetration distance. No greater penetrations were present in that area.

In specimen 5D, fatigue pores were observed in copper, but decreasing toward the interface. There were almost no pores in the diffusion zone. No pores were observed in brass. The particular area used for evaluation of the penetration distance was free from pores and cracks.

Metallographic investigations of the cross-section of specimen 8D revealed extensive grain-boundary cracks throughout the copper including the diffusion zone (Figure 14). It was also observed that penetration of zinc in the vicinity of such cracks was greater (Figure 18). Zinc has also penetrated extensively along a few boundaries without voids (Figure 18). However, such cases were rare. Some pores were observed along grain boundaries in brass. The area used for evaluation contained regions of greater penetration along grain boundaries.

Specimen 4D revealed neither grain-boundary cracks and pores, nor abnormal penetration of zinc. No pores were observed in brass.

Investigations of specimen 7D revealed only one or two cracks in the grain boundaries in the diffusion zone and there were very few fatigue pores in the copper (Figure 15). No fatigue pores were observed in brass.

The values of the penetration distance "x" together with values of x^2/t and log x^2/t are given in Table 4.

4. DISCUSSION AND ANALYSIS

The average penetration distance "x" in each sample was obtained from the measured area by division by the length of the diffusion zone considered for area measurement. The values of x^2/t, a quantity proportional to D, are tabulated in Table 4, together with values of log x^2/t.

From the slope of a plot of log x^2/t versus 1/T, the activation energy for the diffusion process can be obtained. Such a plot is given in Figure 22.

The plot consists of two straight lines, one corresponding to the low temperature grain-boundary diffusion predominant range (below 565°C), and the other to the higher temperature range, where volume diffusion is the controlling factor. The value of the activation energy at temperatures above 565°C as obtained by this method is 39,500 ± 5,900 cals/gmole. Table 6 shows that this is in good agreement with data reported in the literature. For the low-temperature region, where grain boundaries play the predominant role, the activation energy is found to be 16,680 cals/gmole. However, data for grain-boundary diffusion are very few and a direct comparison may not be possible because the activation energy for grain-boundary diffusion may vary from 23,000 cals/gmole to even negative values (60), depending on the misorientation angle.

Let us now consider the individual tests separately. Specimens 6S and 6D were both annealed at 500°C for one week. The ratio of dynamic diffusivity to static diffusivity $[(x^2/t)_D/(x^2/t)_S]$ is 1.17. There is thus a slight effect of fatigue cycling on diffusion rate at this temperature and testing time. Although there were one or two cracks in the whole

cross-section in the diffusion zone, the particular area chosen for measurement of area was free from any such cracks. Therefore this observed enhancement by a factor of 1.17 should be due to structural changes associated with fatigue other than observed cracks, such as sub-cells or pores of submicroscopic size. The probability that the enhancement could be due to cracks present in the specimen, but not appearing on the cross-section, cannot be ruled out. However, this enhancement in this particular sample shows that it can occur without a visible microscopic crack or pore. It should be kept in mind that at this temperature grain-boundary diffusion has a predominant role to play in diffusion.

In the specimens tested at 550°C, namely 9S and 9D, for 120 hours, the ratio of dynamic diffusivity to static diffusivity $[(x^2/t)_D/(x^2/t)_S]$ is 1.05. There seems to be a slight effect of fatigue cycling at this temperature and time also. There were no grain boundaries with pores in the measured area. This slight enhancement, although insignificant quantitatively, should be therefore due to structural changes associated with fatigue. Again this temperature falls in the region where grain-boundary diffusion is predominant.

Let us consider the tests conducted at 595°C and 593°C together, since the temperature difference is negligibly small. Specimen 5D was run for 52 hours and 8D for 69 hours to find out any effect of time on cycling on the observed dynamic diffusivity. The fact that the point corresponding to 5D falls almost on the log x^2/t versus 1/T plot indicates that there is no significant enhancement observed in this case. The point corresponding to 8D falls well above that corresponding to 8S. The ratio of dynamic diffusivity to static diffusivity $[(x^2/t)_D/(x^2/t)_S]$ is 1.235. Thus for the same conditions as for 5D, but for prolonged cycling, there is an enhancement of the diffusivity by a factor of 1.235. This should therefore be caused by

structural changes associated with prolonged fatigue cycling. Greater penetration of zinc along grain boundaries with pores and cracks was present in the measured area. The enhancement is thus due to enhanced diffusion along grain boundaries (Figure 18). The specimen, however, revealed greater penetration along grain boundaries even without pores (Figure 18). Thus the voids may develop later and further enhance diffusion. However, such high penetrations without pores were very few. They can be attributed to a possible combination of the right amount of fatigue damage accumulated and suitable grain misorientations.

Considering specimen 4D (630°C, 13 hours), we find that there is no observed effect at this temperature and for this selected testing time.

At 704°C (specimens 7S and 7D) the ratio of the dynamic diffusivity to static diffusivity $[(x^2/t)_D/(x^2/t)_S]$ is 1.04, or close to one. Thus there seems to be only a small effect of fatigue cycling at this temperature on diffusion. However, even though this ratio falls on the scatterband of data, it may be due to enhancement of grain-boundary penetration in the area measured. There were extremely few fatigue pores in the specimen.

These observations led to the conclusion that fatigue strain cycling increases the observed diffusivity beyond a certain number of cycles by enhancing grain-boundary diffusion. There is evidently greater penetration along grain boundaries associated with observable microscopic pores and cracks. There is also a preparatory stage in fatigue damage accumulation, after which enhanced grain-boundary penetration occurs.

In trying to explain the enhancement of observed diffusivity caused by fatigue cycling after a certain stage (possibly that of

submicroscopic grain-boundary damage), the mechanisms of high temperature fatigue damage accumulation and of structural changes accompanying it should be considered.

Wood et al. (61) have reported that room-temperature fatigue damage occurs mainly by two mechanisms, depending on the strain amplitude. They are:

1. sub-cell and subsequent pore formation at the sub-cell boundaries in the case of high strain amplitudes, and
2. slip-band cracking at lower strain amplitudes.

Ronay et al. (62) have reported that at temperatures above 400°C in copper and brass, fatigue damage occurs only at grain boundaries. Present observations at still higher temperatures are in agreement with these findings.

Thus for an amplitude of strain, for which damage occurs by slip-band cracking at room temperature, grain-boundary cracking occurs at high temperatures.

Allen and Forest (63) proposed that high-temperature fatigue is similar to creep. Freudenthal (64) reasoned that long-life high-temperature fatigue was similar to creep with respect to mechanisms. Thus all reports including the present observations converge to a single point, namely, grain-boundary damage at high demperatures. It is necessary to consider this in more detail to explain the observations.

According to Ronay et al. (62) uniform deformation, as applied to a polycrystalline metal, is transmitted internally to individual grains in an inhomogeneous manner. For example, in low temperature fatigue it concentrates on slip zones under small strain amplitudes and at sub-cell boundaries at high strain amplitudes. Thus the amount of accumulated

deformation is higher in such regions and therefore damage begins in them. The same concept of "abnormal strain" was introduced by Wood et al. (61).

The progress of grain-boundary damage leading to pores is explained in various ways by different investigators.

Let us consider how fatigue damage at sub-cell boundaries or slip bands at room temperature changes to grain boundaries at high temperatures. There are two possible explanations.

Firstly, according to Ronay et al. (49), at high temperatures slip in a grain becomes dispersed so that only grain boundaries remain as potential zones of abnormal strain. With continued cycling, the irreversible strain accumulates at grain boundaries. After a certain number of cycles depending on temperature, strain amplitude, and misorientation, the irreversivle strain accumulated restricts the slip of adjacent grains. Due to such a strain incompatibility, damage occurs in the grain boundaries.

Secondly, Feltner and Laird (65) report that fatigue damage is equivalent to unidirectional straining. Low strain-amplitude fatigue is similar to stage I of unidirectional straining and high strain-amplitude fatigue to stage II of unidirectional straining. On the basis of observations made on high-amplitude tests at 78°K and 300°K at different high strain amplitudes, the authors report that in f.c.c. metals such as copper the fatigue deformation causes the sub-cells. The size of the sub-cell is a function of the temperature and strain amplitude only. It increases with increase in temperature and with decrease in strain amplitude. It can be argued on this basis that at temperatures above 400°C, the cell size coincides with the grain size and the lower strain-amplitude limit for the high strain-amplitude region reaches zero value. Thus damage occurs at grain boundaries. According to Feltner and Laird, cell walls consist of

tangled dislocations and interspersed dislocation loops. With increasing temperature there are more tangled dislocations. They vary from simple tilt boundaries to more complex mixed dislocation boundaries. At smaller strain amplitudes the dislocation pattern consists mainly of dislocation dipoles. Then, at high temperatures, there should be an "effective grain-boundary thickening" since cell walls coincide with original grain boundaries. In other words, there is an increase in the dislocation concentration in and around the grain boundaries as a result of fatigue cycling. The accumulation of dislocations can give rise to voids or pores, which either increase in size or link by multiplication to form bigger cracks. However, the amount of damage accumulated and the time for initiation of pores or voids will depend on the misorientation of the adjacent grains also. The possible ways by which accumulation of dislocations can give rise to grain-boundary cracks are explained in detail by Smith and Barnby (66). Although their explanation is for "nucleation of grain-boundary cavities during high-temperature creep," they could equally be valid for the present case because conditions such as high temperature, low stresses, and pile-up of dislocations are common to both.

Grain-boundary sliding and grain rotation may also be important in cavity formation. This may explain the surface irregularities such as intrusions and extrusions, common to fatigue deformation, even at high temperatures. Nucleation of cavities due to grain-boundary sliding may arise from the opening of voids and non-wetting inclusions or at irregularities in the boundary.

In the light of the above theories, it follows that at the high temperatures used for the diffusion experiments, fatigue deformation accumulates progressively at grain boundaries. The accumulation of dislocations at

grain boundaries and "effective grain boundary thickening" will enhance grain-boundary diffusion. But this enhancement becomes significant only after a particular stage in fatigue damage progress has been reached. This stage may possibly be associated with some kind of submicroscopic damage such as sub-cell formation and the initiation of pores or voids along grain boundaries. The number of cycles required for this stage to reach depends on temperature, strain amplitude, the number of slip systems operating under these conditions, and grain misorientation. At high temperatures, grain-boundary diffusion is not predominant; any enhancement of observed diffusivity may therefore be only apparent or only along grain boundaries. The latter can occur only after sufficient fatigue damage progress has been made. This explains why the observed enhancement is only in specimen 8D and not in 5D. The observations that pronounced enhanced diffusion has occurred only along a few grain boundaries, can be explained by the fact that a sufficient progress in fatigue damage has been made only along them due to suitable misorientations between the adjacent grains. Of course, microscopic cracks will further enhance diffusion along grain boundaries.

At lower temperatures, where grain-boundary diffusion is predominant and affects overall diffusivity, a real and significant enhancement of the diffusivity can occur after sufficient fatigue damage has been accumulated. This explains the enhancement observed in specimen 6D. But even at these temperatures, the enhancement can only be insignificant until and unless sufficient fatigue damage has been accumulated. This explains the insignificant enhancement observed in specimen 9D.

The enhancement observed in 7D, although very small, is only due to enhanced penetration along a cracked grain boundary in the measured area.

It is also evident that volume diffusion is not affected by fatigue cycling to any measurable degree.

The observed grain-boundary damage in fatigued samples confirms the already reported fact that at high temperatures, fatigue damage accumulates at grain boundaries. The damage starts in the form of pores, which either link by multiplication or grow into cracks.

The fact that there is no noticeable enhancement of diffusion until after sufficient fatigue damage has been accumulated, indicates that either the vacancies generated during high-temperature fatigue are too small in number or too short-lived to affect diffusion.

Since no abnormal fatigue pores or cracks were observed in the diffusion zone of brass, vacancies seem to have little part in causing fatigue damage. Thus the "vacancy clustering mechanism" of fatigue damage stands still in doubt. At least it is definite that the extra vacancies, generated by nonuniform diffusion, are not participating in fatigue damage to any observable degree.

Fatigue cracks did occur in the grain boundaries in the diffusion zone, although rarely. Their limited occurrence in comparison with other regions in the copper is more likely due to the lower strain amplitude and strain rate in this region than to the exhaustion of vacancies by the diffusing zinc atoms.

It is known that at temperatures lower than 400°C, fatigue damage accumulates in the grains (62). Then it follows that under those temperature conditions, volume diffusion may be enhanced after sufficient fatigue damage has been accumulated, just as the observed grain-boundary enhancement at high temperatures. Of course, it may be difficult to notice this because of the low diffusion rates at low temperatures.

5. CONCLUSIONS

On the basis of the observations, it is concluded that in the copper-zinc diffusion system for the conditions of strain cycling and temperatures used,

1. Fatigue strain cycling has no noticeable effect on volume diffusion.
2. Strain cycling affects grain-boundary diffusion to some extent, but only after sufficient fatigue damage has been accumulated. This stage is possibly associated with the formation of subcells and/or submicroscopic pores or voids.
3. The effect on grain-boundary diffusion affects the overall diffusivity at temperatures where grain-boundary diffusion is predominant. At higher temperatures, the effect is confined to grain boundaries only.
4. The overall effect of strain cycling is therefore expected to increase with a decrease in temperature in the grain-boundary diffusion predominant range. However, below about 400°C, the effect would be reduced because the fatigue mechanism is no longer restricted to grain boundaries. Volume diffusion, however, would be enhanced below about 400°C, after sufficient fatigue damage has been accumulated.
5. A mechanism, alternate to "strain incompatibility at grain boundaries," is suggested for high-temperature or grain-boundary damage. At these temperatures, the mechanism is similar to that at low temperatures and high strain amplitudes, but only

the sub-cell size has increased to become the same as the grain size.

BIBLIOGRAPHY

1. Konobeevski, S.T., and Selisski, J. Phys. Zeit. der Sowjetunion, v. 4, 1933, p. 459.

2. Nachtrieb, N.H., Weil, J.A., Catalano, E., and Lawson, A.W. "Self Diffusion in Solid Sodium II--The Effect of Pressure." J. Chem. Phys., v. 20, 1952, p. 1189.

3. Nachtrieb, N.H., and Lawson, A.W. "Effect of Pressure on Self Diffusion in White Phosphorus." J. Chem. Phys., v. 23, 1955, p. 1193.

4. Nachtrieb, N.H., Resing, H.A., and Rice, S.A. "Effect of Pressure on Self Diffusion in Lead." J. Chem. Phys., v. 31, 1959, p. 135.

5. Liu, T., and Drickamer, H. "The Effect of Compression and of Hydrostatic Pressure on the Diffusion of Anisotropy in Zinc." J. Chem. Phys., v. 22, 1954, 0. 312.

6. Tichelaar, G., and Lazarus, D. "Effect of Pressure on Anelastic Relaxation in Silver-Zinc System." Phys. Rev., v. 113, 1959, p. 438.

7. Hudson, J.B., and Hoffman, R.E. "The Effect of Hydrostatic Pressure on Self Diffusion in Lead." Trans. AIME, v. 221, 1961, p. 761.

8. Fastov, N.S. "Features of the Thermodynamics of Solid Solutions." Physics of Metals and Metallography (Translation), v. 7, no. 3, 1959, p. 32.

9. Machlin, E.S. "Role of Strain-Energy in Solid Solution Thermodynamics." Trans. AIME, v. 220, 1954, p. 592.

10. Oriani, R. A. "Thermodynamics of Liquid Ag-Au and Au-Cu Alloys and the Question of Strain-Ageing in Solid Solutions." Acta Met., v. 4, 1956, p. 15.

11. Hultgreen, R. "Misfit Strain Energy in Au-Cu System." Trans. AIME, v. 209, 1957, p. 1240.

12. Fastov, N.S. Doklady Akad. Nauk., S.S.S.R., v. 85, 1952, p. 67.

13. Aleksandrov, L.N., and Lyubov, B.Ya. "Influence of Concentration Stresses on the Rate of Lateral Growth of Pearlite Grains." Doklady Akad. Nauk., S.S.S.R., v. 74, 1950, p. 1081.

14. Dienes, G.J., and Damask, A.C. "Radiation Enhanced Diffusion in Solids." J. Ap. Phys., v. 29, 1958, p. 1713.

15. Andreeva, A.G., Kontorovich, I.E., and Sovalova, A.A. "Influence of Grain Size on Diffusion of Nitrogen in Iron." Zhur. Tekh. Fiz., vol. 17, 1947, p. 1521.

16. Buffington, F.S., and Cohen, M. "Self Diffusion in Alpha Iron under Uniaxial Compressive Stress." J. of Metals, v. 4, 1952, p. 859.

17. Brown, A.F., and Blackburn, D.A. "Apparent Enhancement of Diffusion Coefficients in Plastically Deformed Metals." Acta Met., v. 11, 1953, p. 1017.

18. Dekhtyar, I.Ya., and Mikhalenkov, V.S. "Effect of Plastic Deformation on Diffusion Rate in Ni-Mo Alloys." Ukrain. Phiz. Zhur., Akad. Nauk., U.R.S.R., v. 3, no. 3, 1958, p. 385.

19. Forestieri, A.F., and Girifalco, L.A. "The Effect of Plastic Deformation on Self-Diffusion in Silver." J. Phys. Chem. Solids, v. 10, 1959, p. 99.

20. Lee, C.H., and Maddin, R. "The Effect of Torsional Strains on Self Diffusion in Silver Single Crystals." Trans. AIME, v. 215, 1959, p. 397.

21. Shestopalov, L.M., and Romashkin, Y.P. "Diffusion of Silver in Plastically Deformed Copper." Sov. Phys. Solid State, v. 2, no. 12, 1961, p. 2664.

22. Darby, Jr., J.R., Tomizuka, C.T., and Balluffi, R.W. "Self Diffusion in Silver during Plastic Deformation in Extension and Compression." J. Ap. Phys., v. 30, 1959, p. 104.

23. Chollet, P., Grosse, I., and Philibert, J. "On the Influence of a Plastic Deformation on Rate of Intermetallic Diffusion." C.R. Acad. Sci., Paris, v. 252, 1961, p. 728.

24. Barry, B.A., and Brown, A.F. "Self-Diffusion in Silver during Torsional Deformation." Acta Met., v. 12, 1964, p. 209.

25. Killpatrick, D.H., and Balluffi, R.W. "Diffusion Rates in Face Centred Cubic Copper Alloys during Torsional Deformation." Acta Met., v. 11, 1963, p. 439.

26. Duhl, D., Taranto, J., and Cohen, M. "Discussion on Apparent Enhancement of Diffusion in Plastically Deformed Metals." Acta Met., v. 12, 1964, p. 678.

27. Balluffi, R.W., and Ruoff, A.F. "On Strain-Enhanced Diffusion in Metals. I--Point Defect Models." J. Ap. Phys., v. 34, 1963, p. 1634.

28. Balluffi, R.W., and Ruoff, A.F. "On Strain-Enhanced Diffusion in Metals. II--Dislocation and Grain-boundary Short-Circuiting Models." J. Ap. Phys., v. 34, 1963, p. 1848.

29. Balluffi, R.W., and Ruoff, A.F. "On Strain-Enhanced Diffusion in Metals. III--Interpretation of Recent Experiments." J. Ap. Phys., v. 34, 1963, p. 2862.

30. Wazzan, A.R., Mote, J., and Dorn, J.E. ASTIA 257188, April 18, 1961.

31. Brown, A.F. "The Effect of Vibrational Deformation on Diffusion-Controlled Reactions in Metals." Applied Materials Research, v. 5, 1966, p. 67.

32. Shepard, O.C., and Sherby, O.D. "Influence of Strain on Diffusion and Diffusion-Controlled Processes." AEC, Stanford University, Stanford, California, 1966.

33. Forsyth, P.J.E. "Some Observations on the Nature of Fatigue Damage." Phil. Mag., v. 2, 1957, p. 437.

34. Broom, T., Molineux, J.H., and Whittaker, V.N. "Structural Changes during the Fatigue of Some Al Alloys." J. Inst. Met., v. 84, 1955-56, p. 357.

35. Laird, C., and Thomas, G. "On Fatigue-Induced Reversion and Overageing in Dispersion Strengthened Alloy Systems." Ford Motor Co. Publication, Jan. 18, 1967.

36. Fairbanks, H.V., and Dewiz, Jr., F.J. "Effects of Acoustical Waves on the Annealing of Steels." J. acoust. Soc. Am., v. 28, 1957, p. 588.

37. Blaha, F., and Langenecker, B. "Plastizitätsuntersuchungen von Metallkristallen in Ultraschallfeld." Acta Met., v. 7, 1959, p. 93.

38. Hirsch, P.B. "Extended Jogs in Dislocations in F.C.C. Metals." Phil. Mag., v. 7, 1962, p. 67.

39. "Fatigue--An Interdisciplinary Approach." Ed.: Burke, J.J., Reed, N.L., and Weiss, V. Syracuse Univ. Press, 1964, p. 4 and p. 43.

40. Mott, N.F. "Slip at Grainboundaries and Grain-Growth in Metals." Proc. Phys. Soc. (London), v. 60, 1948, p. 391.

41. "Mechanical Behaviour of Materials at Elevated Temperatures." Ed.: Dorn, Univ. of California Engg. Extension Series, McGraw-Hill Inc., 1961, p. 131 and p. 141.

42. Atkinson, H.H. "Small-Angle Scattering of X-Rays and Neutrons from Deformed Metals." J. Ap. Phys., v. 30, 1959, p. 637.

43. Thomas, K., and Franks, A. "Study of X-Ray Scattering from Fatigued Metals." J. Ap. Phys., v. 30, 1959, p. 649.

44. Grosskruetz, J.C., and Rollins, F.R. "Small Angle X-Ray Scattering from Fatigued Metals." J. Ap. Phys., v. 30, 1959, p. 649.

45. Guinier, A., and Format, G. "Small Angle Scattering of X-Rays." John Wiley and Sons, N.Y., 1955, pp. 195-213.

46. Antal, J.J., Weiss, R.J., and Dienes, G.J. "Long-Wavelength Neutron Transmission as an Absolute Method for Determining the Concentration of Lattice Defects in Crystals." Phys. Rev., v. 99, 1955, p. 1081.

47. McCammon, R.D., and Rosenberg, H.M. "The Fatigue and Ultimate Tensile Strengths of Metals Between 4.2°and 293°K." Proc. Roy. Soc., v. 242, 1957, p. 203.

48. Maccrone, R.K., McCammon, R.D., and Rosenberg, H.M. "The Fatigue of Metals at 1.7°K." Phil. Mag., v. 4, 1959, p. 267.

49. Ronay, M. "On Strain-Incompatibility and Grain-boundary Damage in Fatigue." Tech. Report No. 9, Inst. for the Study of Fatigue and Reliability, Columbia Univ., N.Y., 1964.

50. Wood, W.A., and Nine, H.D. "Differences in Fatigue Behaviour of Single Copper Crystals and Polycrystalline Copper at Elevated Temperatures." Tech. Report No. 15, Inst. for the Study of Fatigue and Reliability, Columbia Univ., N.Y., 1964.

51. Grosskruetz, J.C., Reiman, W.H., and Wood, W.A. "Correlation of Optical and Electron-Optical Observations in Torsion Fatigue of Brass." Tech. Report No. 19, Inst. for the Study of Fatigue and Reliability, Columbia Univ., N.Y., 1964.

52. Riggs, B.A. "A Consideration of Diffusion in Strained Systems." Acta Met., v. 12, 1964, p. 952.

53. Adler, Isidore. "X-Ray Emission Spectrography in Geology." Amsterdam, N.Y., Elsevier Pub. Co., 1966, pp. 201-217.

54. Crank, J. "The Mathematics of Diffusion." Clarendon Press, Oxford, 1956, pp. 46 and 63.

55. Balluffi, R.W., and Seigle, L.L. "Diffusion in Bimetal Vapor-Solid Couples." J. Ap. Phys., v. 25, no. 5, 1954, p. 607.

56. Guy, A.G. "Elements of Physical Metallurgy." Addison Wesley Publishing Co., Reading, Mass., U.S.A., 1959, p. 409.

57. Resnick, R., and Balluffi, R.W. "Diffusion of Zinc and Copper in Alpha and Beta Brasses." J. of Metals, 1955, p. 1004.

58. da Silva, L.C.C., and Mehl, R.F. "Interface and Marker Movements in Diffusion in Solid Solutions of Metals." Trans. AIME, v. 191, 1951, p. 155.

59. Horne, G.T., and Mehl, R.F. "Mobilities of Diffusion in Alpha Brass." Trans. AIME, v. 203, 1955, p. 88.

60. Flanagan, R., and Smoluchowski, R. "Grainboundary Diffusion of Zinc in Copper." J. App. Phys., v. 23, 1952, p. 785.

61. Wood, W.A., Cousland, S. McK., and Sargent, K.R. "Systematic Microstructural Changes Peculiar to Fatigue Deformation." Acta Met., v. 11, 1963, p. 643.

62. Ronay, M., Reimann, W.H., and Wood, W.A. "Mechanism of Fatigue Deformation at Elevated Temperatures." Tech. Report No. 7, Inst. for the Study of Fatigue and Reliability, Columbia Univ., N.Y., 1964.

63. Allen, N.P., and Forest, P.G. "Influence of Temperature on the Fatigue of Metals." International Conference on Fatigue, Inst. Mech. Engrs., 1956, p. 327.

64. Freudenthal, A.M. "Aspects of High Temperature Fatigue Damage." Acta Met., v. 11, 1963, p. 753.

65. Feltner, C.E., and Laird, C. "Cyclic Stress-Strain Response of F.C.C. Metals and Alloys--I and II." Acta Met., v. 15, 1967, p. 1621 and p. 1633 respectively.

66. Smith, E., and Barnby, J.T. "Nucleation of Grain-boundary Cavities during High-Temperature Creep." Metal Science Journal, v. 1, 1967, p. 1.

TABLE 1. Data in Literature on Strain-enhanced Diffusion

No.	Authors	Reference	Metal	Tracer or Diffusing metal	Method of Analysis	Temperature °C	Strain Type	Maximum Ds/Du	Minimum $2\sqrt{Dt}$ (μ)
1.	Buffington, Cohen	16	Fe	Fe	Surface Decrease	890	Compression	15	8
2.	Dekhtyar, Mikhalinkov	18	Ni-6% Mo	Co	Absorption	950, 1050, 1150	Compression	1.5	8.5
3.	Forestieri, Girifalco	19	Ag	Ag	Autoradiography	650, 750	Compression	9.1	19 80
4.	Lee, Maddin	20	Ag	Ag	Mechanical Sectioning	700, 800	Torsion	94 78	11 22
5.	Shestapolov, Romashkin	21	Cu	Ag	Chemical Section, Surface Decreases	600	Compression	24	0.2
6.	Darby, Tomizuka, Balluffi	22	Ag	Ag	Mechanical Sectioning	800, 900	Tension, Compression	1	70
7.	Chollet, Grossie, Philibert	23	Fe	Ni	Electronmicroprobe	1200	Torsional Fatigue	1	20
8.	Barry, Brown	24	Ag	Ag	Autoradiography	682	Torsion	1.1	6.8
9.	Killpatrick, Balluffi	25	13% Zn Brass	Zn	Weight loss	809, 707, 657	Torsion	2.1 2.3 3.9	-

TABLE 2

Chemical Composition of OFHC Copper as Received

Spectrographic Analysis

Element	Amount (ppm)
0	3
Ag	10
Fe	1
S	9
As	3
Pl	7
P	1
Sl	4
Bi	0.2
Te	2
Sn	2
Zn	0.5
Ni	3
Hg	1
Cd	0.1
Mn	0.1

Chemical Composition of Brass

Cu	70%
Zn	29.7%
Others	0.3%

TABLE 3. Electron-Microprobe Data

COPPER BRASS DIFFUSION

CU STANDARD EPS 4/1

	Zn	Cu
010.000	0000476	0122025
010.000	0000413	0122184
010.000	0000497	0121495

ZN STANDARD ARL

010.000	0075036	0002052
010.000	0073910	0002005
010.000	0074611	0001110
010.000	0074449	0001089
010.000	0074508	0001082

STANDARD 4D OUTER EDGE OF COPPER RING

010.000	0000458	0121293
010.000	0000467	0121270

TERMINAL POINT OF SCAN (Point 4 on chart)

010.000	0022100	0088115
010.000	0021870	0087228

OTHER TERMINAL POINT OF SCAN (Point 1 on chart)

010.000	0000431	0119617
010.000	0000384	0120194

LEFT EDGE OF TROUGH AS ON CHART RECORD

See Figure 8 for chart.
Applied Voltage = 30 kV.
Take-off angle = 52.5° of x-rays

TABLE 4. Test Data

Specimen Number	6S	6D	8S	8D	5D	4D	5S	4S	7S	7D	9S	9D
Temperature T (°C)	500	500	593	593	595	630	652	670	704	704	550	550
$I/T \times 10^4$	12.95	12.95	11.55	11.55	11.51	11.1	10.82	10.6	10.25	10.25	12.15	12.15
Diffusion-Period, t (hours)	168	168	69	69	52	13	52	13	20	20	120	120
Area* (cm^2)	10.4	11.0	15.3	17.0	13.6	10.0	26.5	16.85	29.5	30.5	12.2	12.5
Diffusion-Penetration, x (μ)	9.2	9.9	13.5	15.0	12.0	8.8	23.4	14.9	26.4	26.9	10.8	11.00
x^2/t	0.502	0.588	2.650	3.270	2.780	6.000	10.540	17.040	34.880	36.290	0.970	1.020
Log x^2/t	$\bar{1}$.7007	$\bar{1}$.7694	0.4233	0.5146	0.440	0.7782	1.0228	1.2315	1.5426	1.5598	$\bar{1}$.9868	0.0086

* On Photograph at Magnification X487.

Length of Diffusion Zone considered as on Photograph at Magnification X487 = 23.25 cm.

TABLE 5. Microstructural Changes of the Dynamic Samples

No.	Type of Feature	Specimens					
		6D	9D	5D	8D	4D	7D
1.	Fatigue pores and cracks in grain-boundaries in Cu	Present. More discontinuous towards interface. Few in Diffusion-Zone.	Few. Only one or two in Diffusion-Zone	Few. More discontinuous towards inter-face. None in Diffusion-Zone	Present. More discontinuous towards inside. Few in Diffusion-Zone	Almost none	Very few
2.	Fatigue pores and cracks in brass	Few	Few	None	Few	None	None
3.	Diffusion voids in brass	Present	Present	Present	Present	Present	Present
4.	Additional	Greater penetra-tion along grainboundaries with cracks	Greater penetration along grain-boundaries with pores	---	Greater penetra-tion along grain-boundaries with and without pores	---	---

TABLE 6. Activation Energy for Diffusion in the Cu-Zn System

Reference	Investigators	Activation Energy, cal./gmole
56	.....	38,000
57	Resnick and Balluffi	40,800
25	Killpatrick and Balluffi	45,170
58	da Silva and Mehl	41,000
59	Horne and Mehl	38,000
..	Present work	39,500

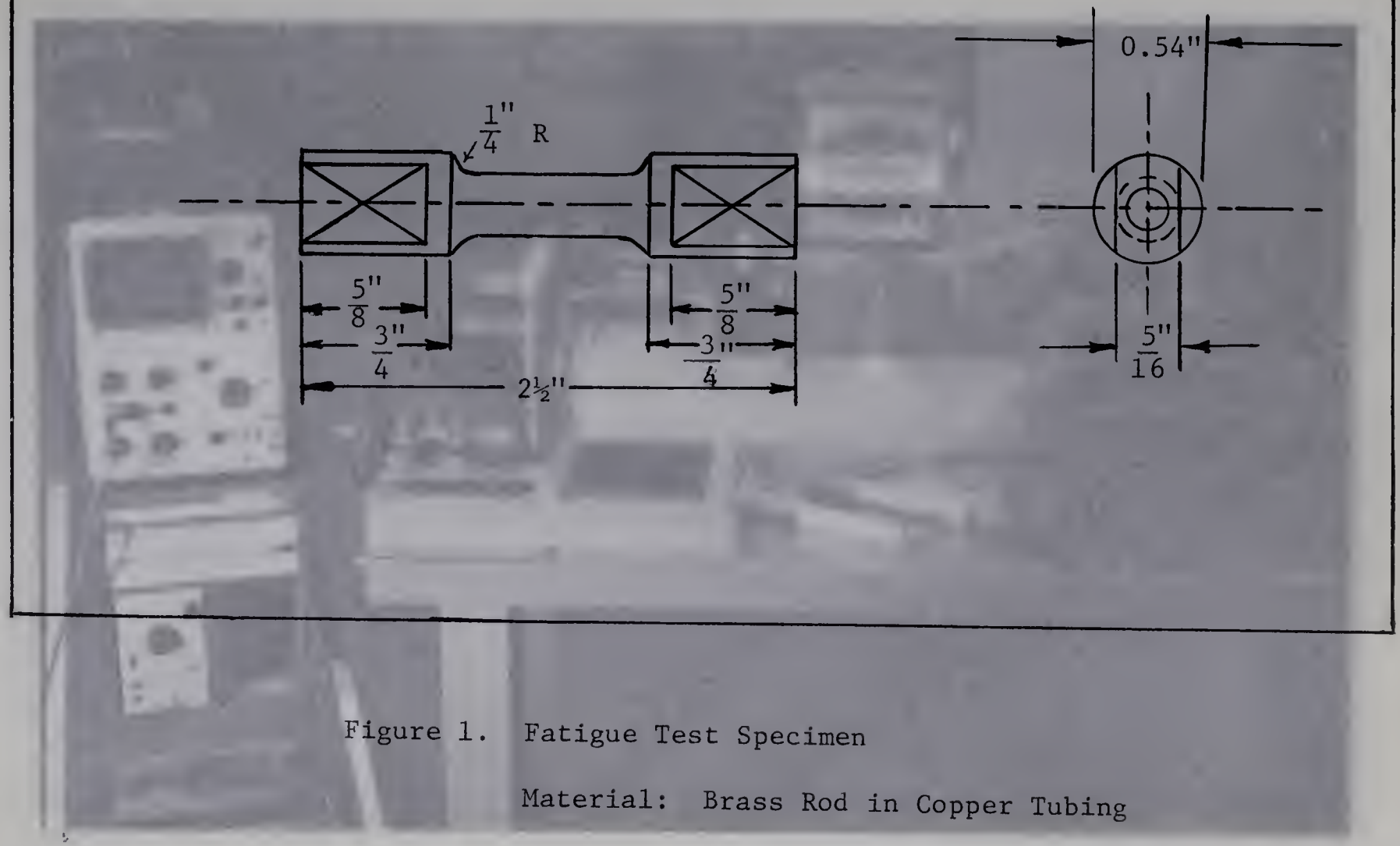

Figure 1. Fatigue Test Specimen

Material: Brass Rod in Copper Tubing

Figure 1. Fatigue Test Specimen

Material: Brass Rod in Copper Tubing

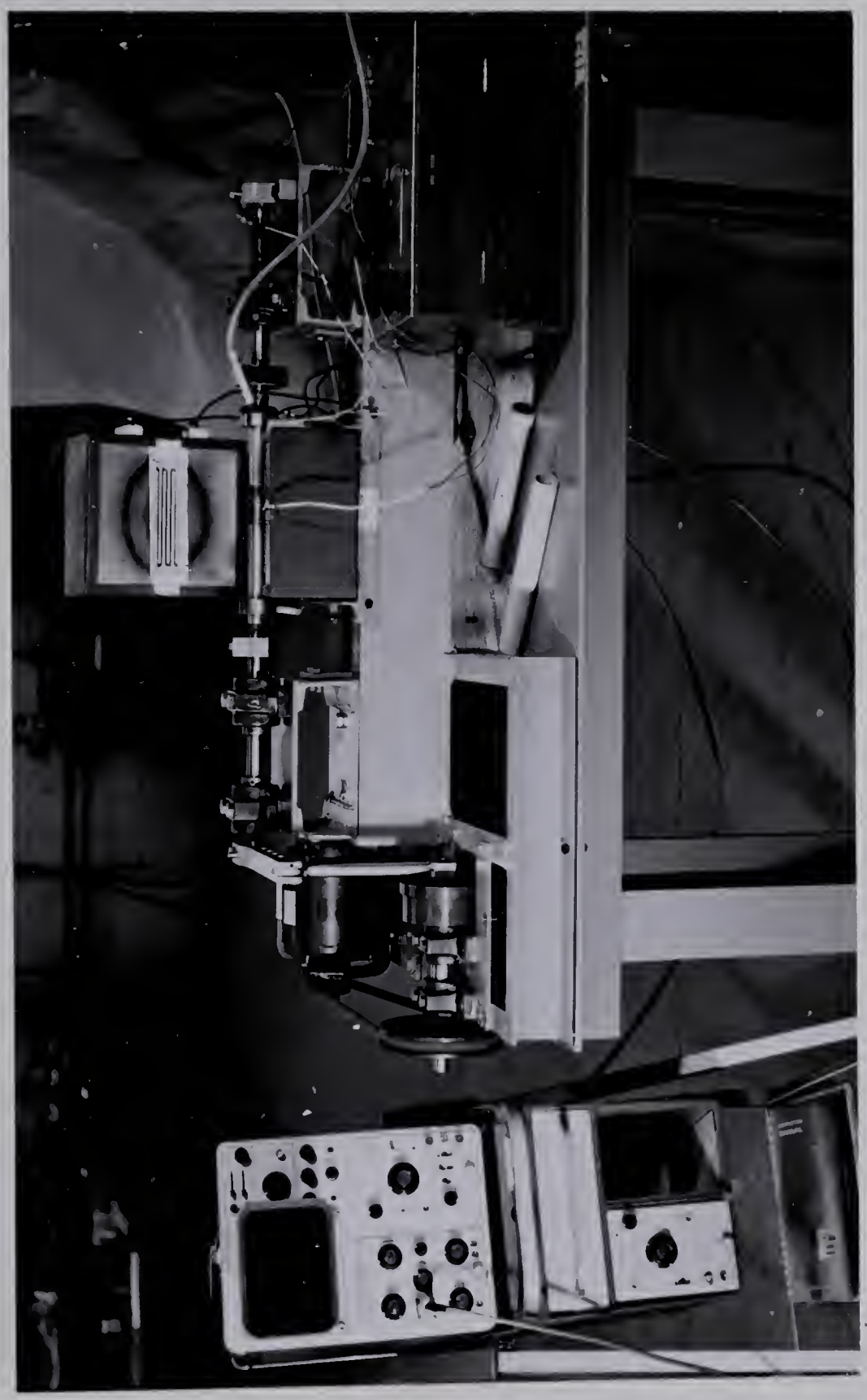

Figure 2. Torsion-Fatigue Testing Machine

Figure 3. Specimen and Grip Assembly

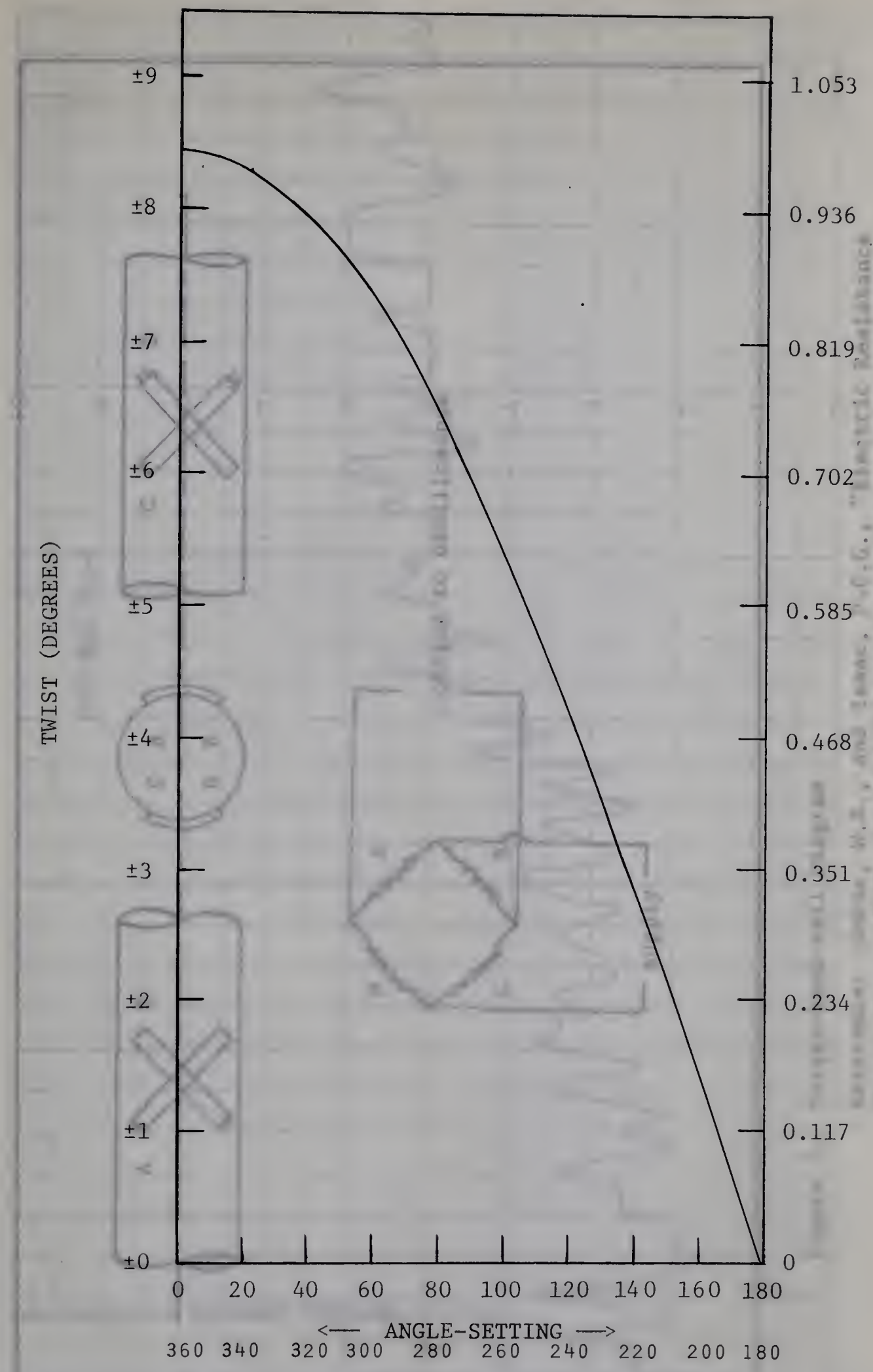

Figure 4. Eccentricity versus Angle of Twist

Figure 4. Eccentricity versus Angle of Twist

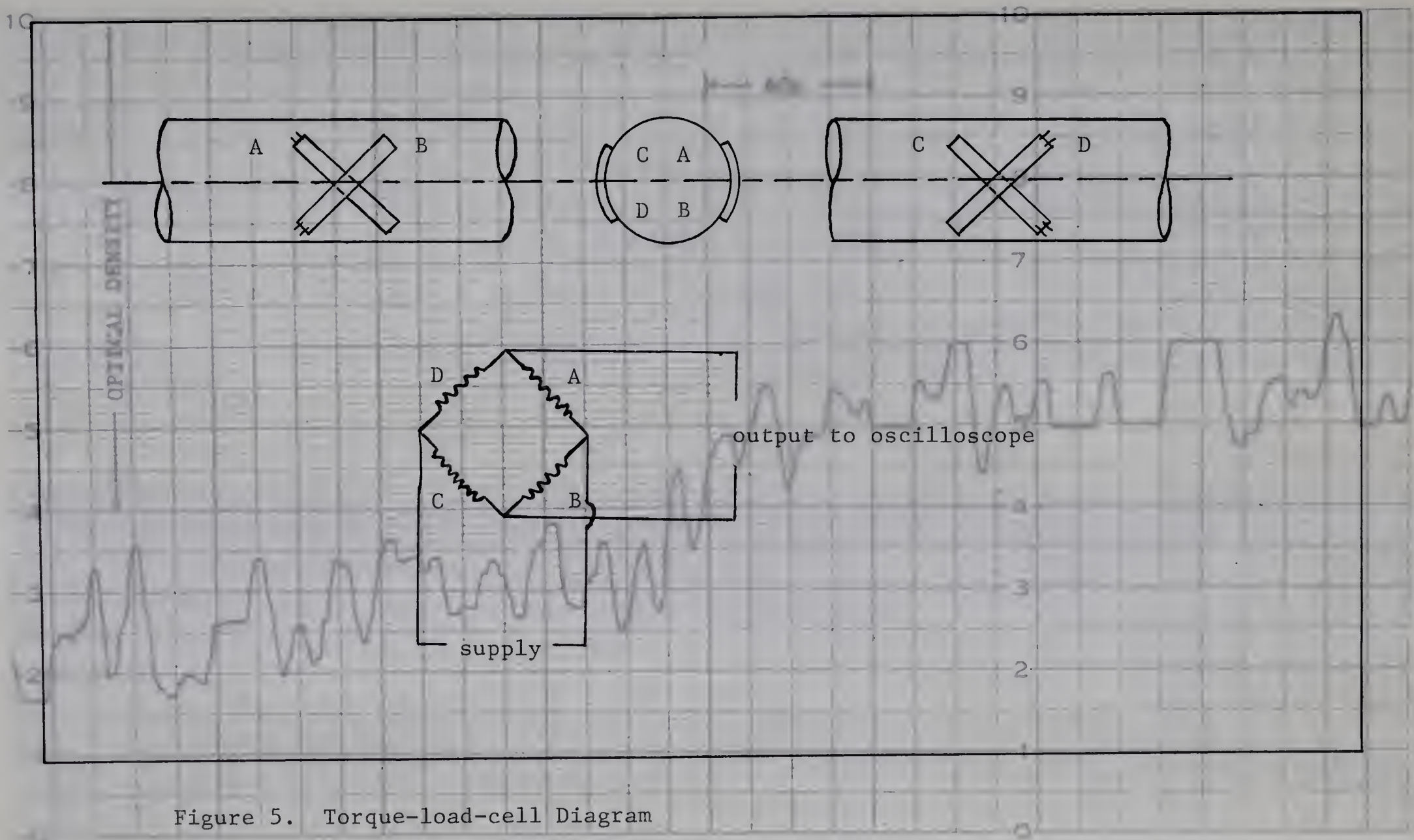

Figure 5. Torque-load-cell Diagram

Reference: Dobie, W.B., and Isaac, P.C.G., "Electric Resistance Strain Gauges," The English Universities Press Limited, London, 1948, p. 94.

Figure 2.- Torque-load-cell Diagram

References: Doyle, W.R., and Isaac, F.C.C., "Electric Resistance Strain Gauges," The English University Press Limited, London, 1948, p. 94.

CAT. NO. 33 01-31

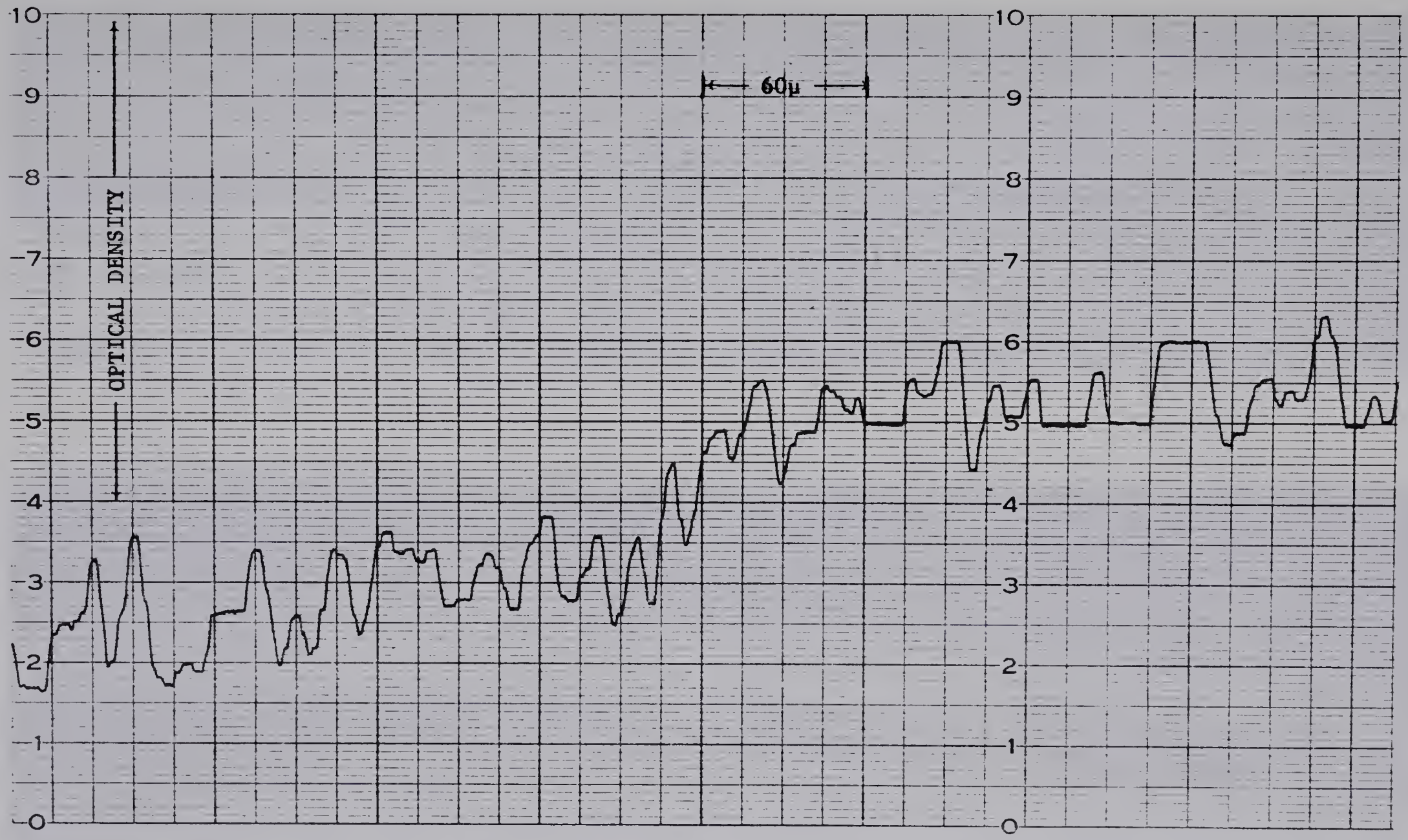

Figure 6. Microdensitometer Traverse of Enlarged X-Ray Microradiograph

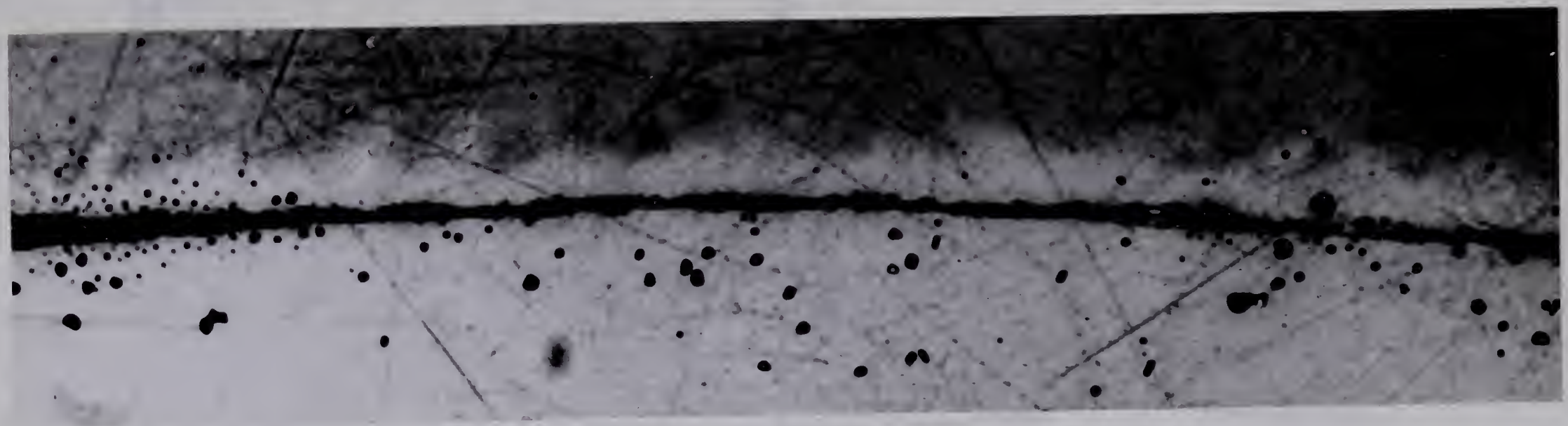

Figure 7. Example of Prints Used for Evaluation: X487

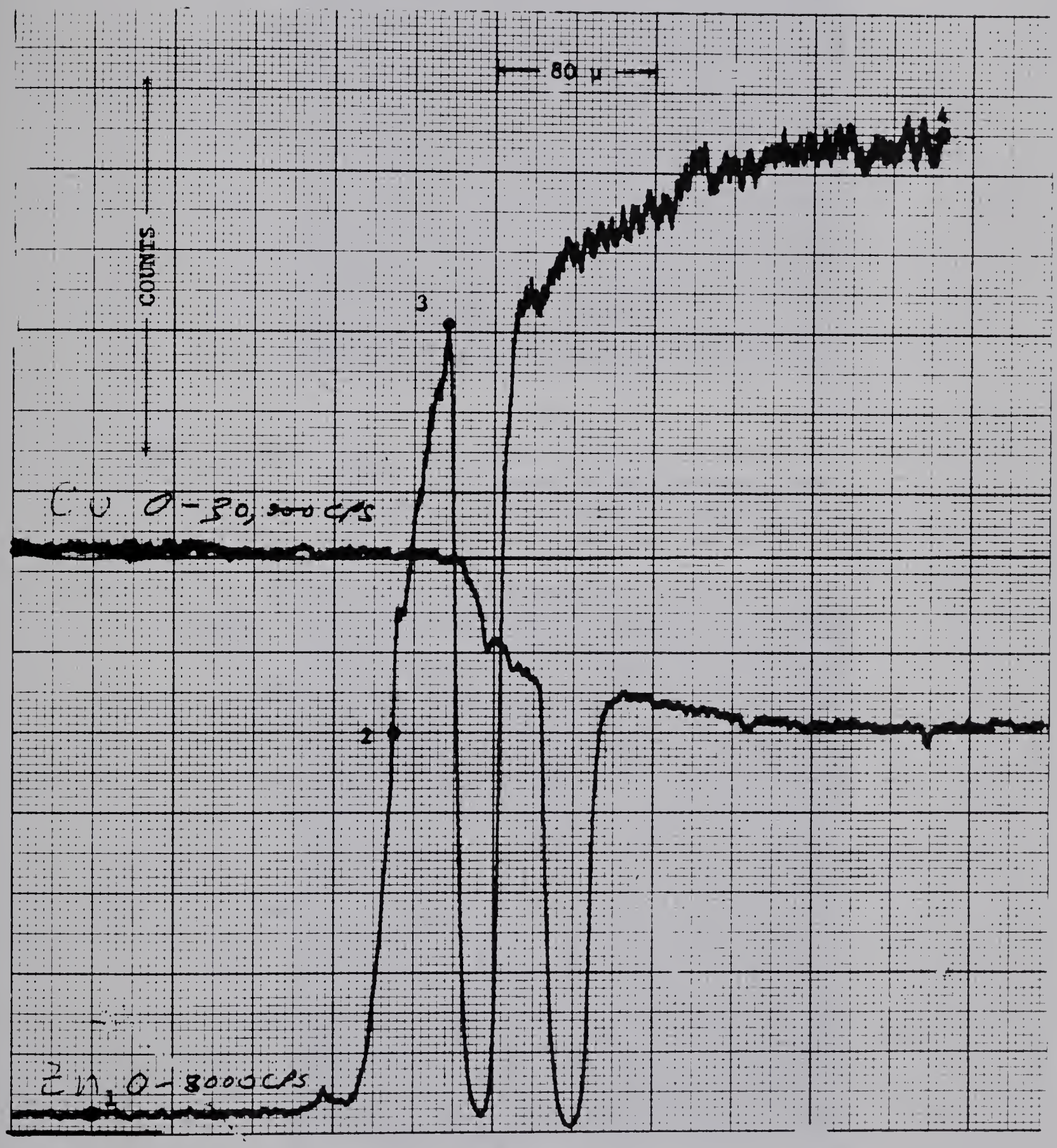

Figure 8. Electron-Microprobe Traverse of Specimen 7S

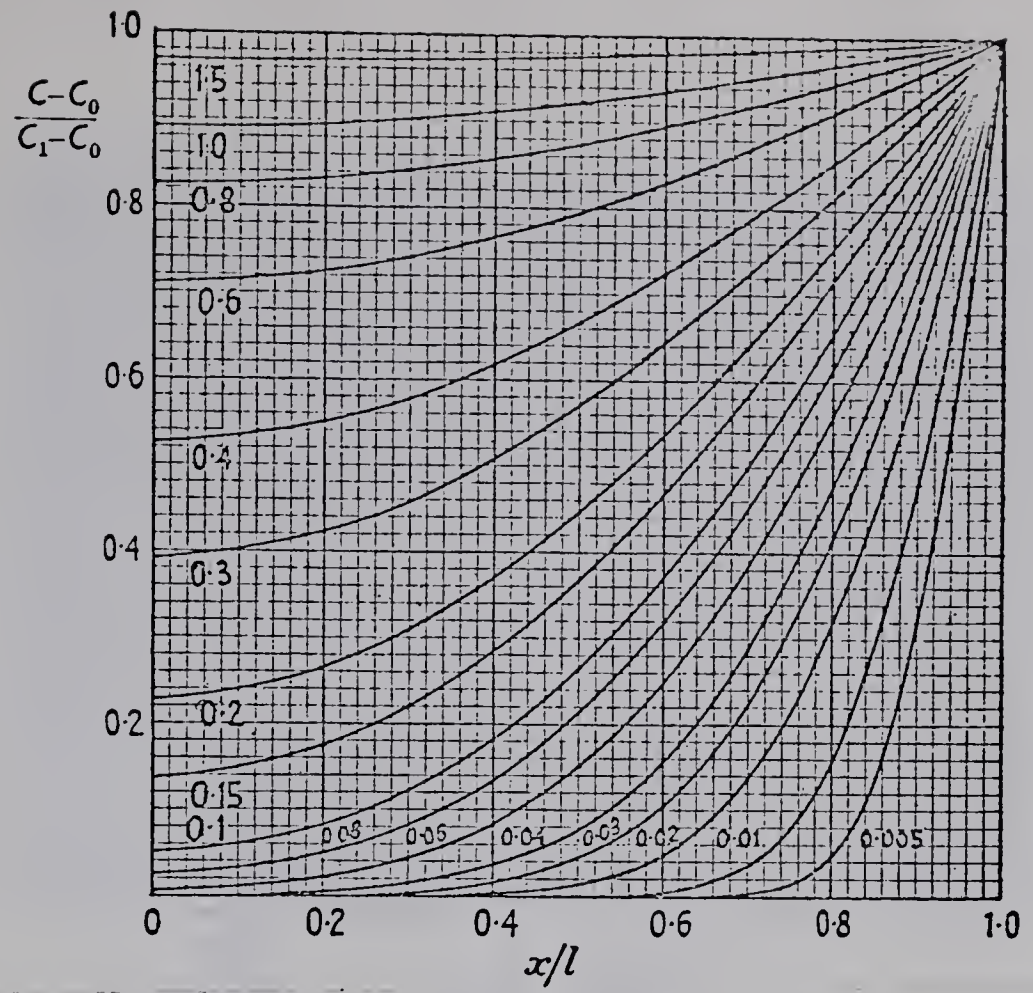

Figure 9(a). Concentration Distributions in the sheet $-\ell < x < \ell$ with initial uniform concentration C_o and surface concentration C_1. Numbers on curves are values of Dt/ℓ^2.

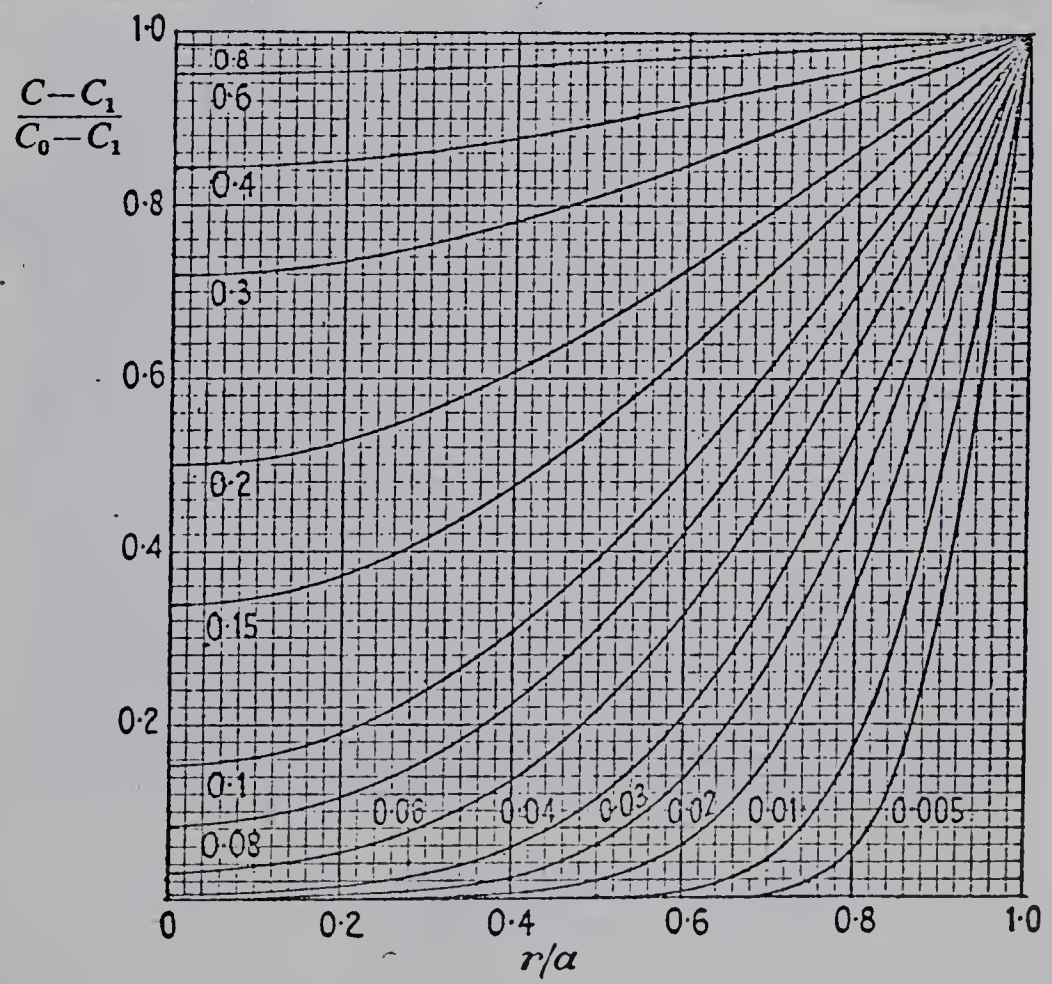

Figure 9(b). Concentration Distributions in solid cylinder with initial concentration C_1 and surface concentration C_o. Numbers on curves are values of Dt/a^2.
Reference: 54.

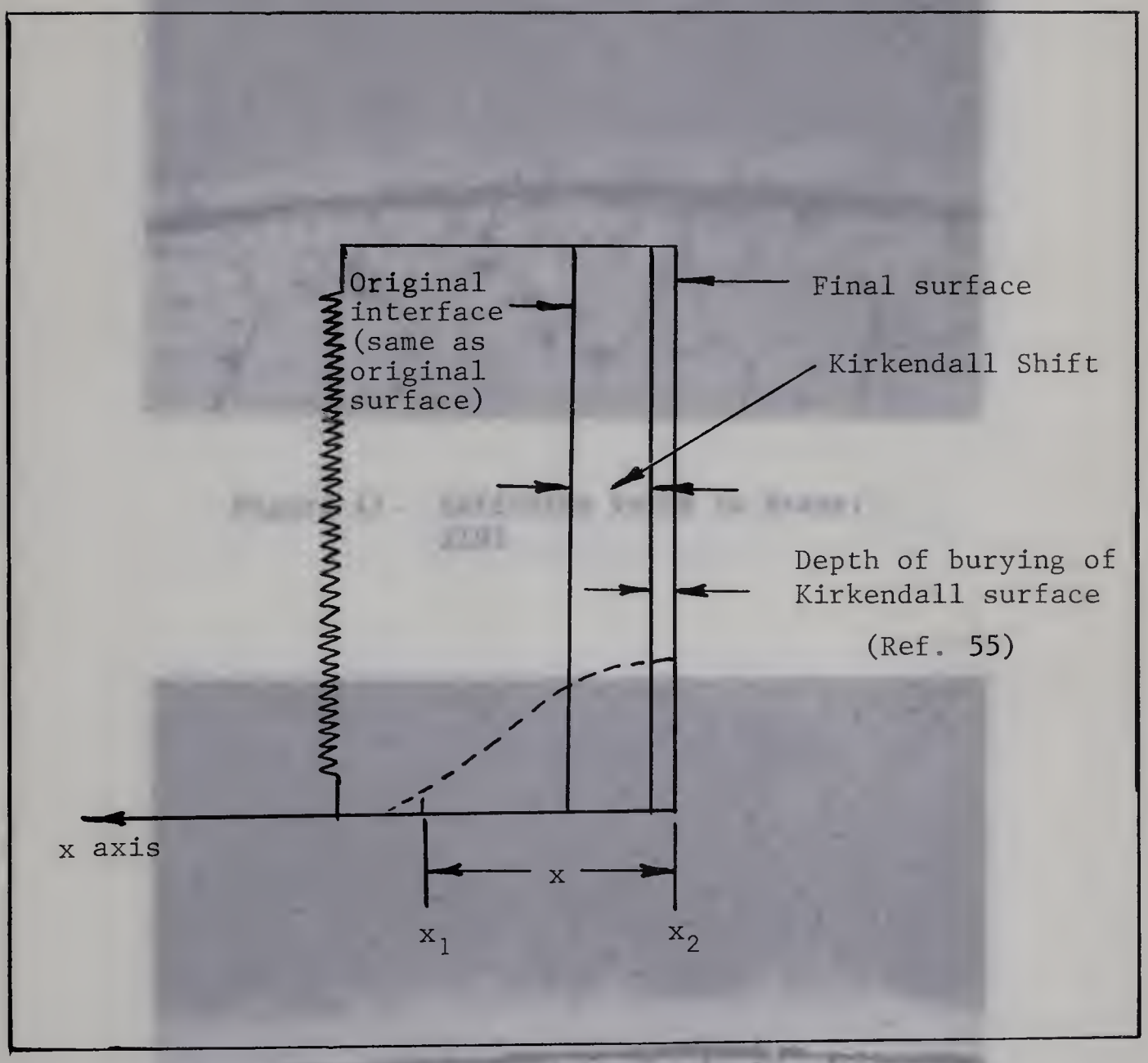

Figure 10. Vapor-Solid Diffusion Couple

Figure 10. Vapor-Solid Diffusion Couple

Figure 11. Diffusion Voids in Brass: X195

Figure 12. Nonuniformity of Diffusion Penetration: X195

Figure 13. Fatigue Cracks at Grainboundaries (Specimen 6D): X75

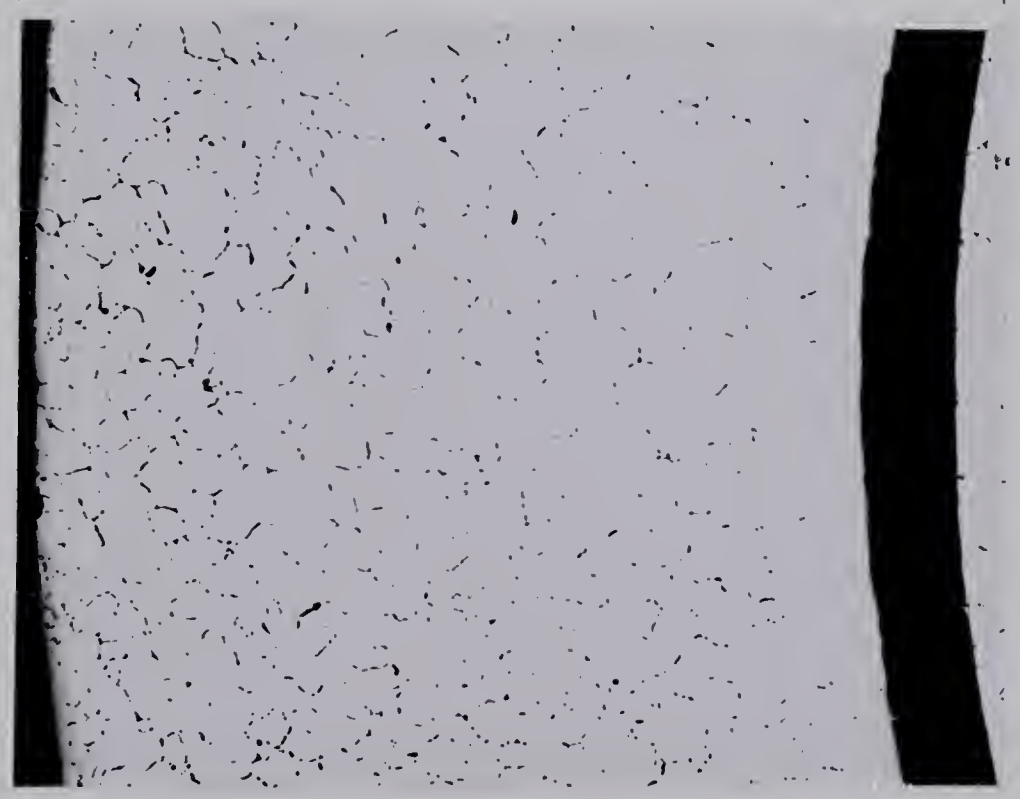

Figure 14. Fatigue Cracks at Grainboundaries (Specimen 8D): X75

Figure 15. Fatigue Cracks at Grainboundaries (Specimen 7D): X75

Figure 16. Fatigue Cracks at Grainboundaries of Brass (Specimen 6D): x75

Figure 17. Greater Penetration along Grain-boundaries (Specimen 6D): X550

Figure 18. Greater Penetration along Grain-boundaries (Specimen 8D): X550

Figure 19. Typical Microstructure of a Dynamic Diffusion Sample: X195

Figure 20. Grainboundary Damage in Copper (unetched): X195

Figure 21. Grainboundary Damage in Copper (etched): X195

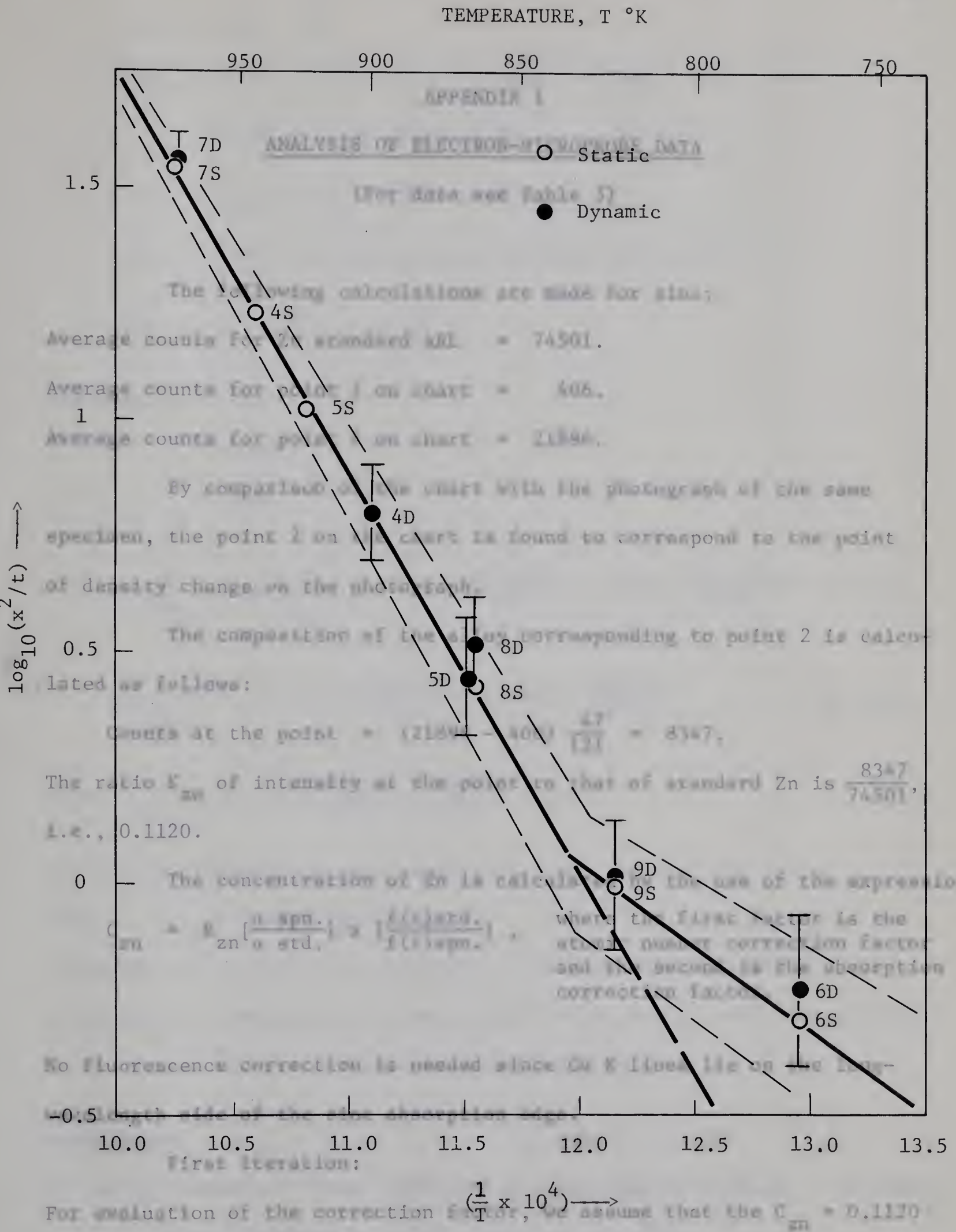

Figure 22. Plot of Log Diffusivity (x^2/t) versus Inverse Test Temperature

Figure 22. Plot of Log Diffusivity (x_2^2/t) versus Inverse Test Temperature

APPENDIX I

ANALYSIS OF ELECTRON-MICROPROBE DATA

(For data see Table 3)

The following calculations are made for zinc:

Average counts for Zn standard ARL = 74501.

Average counts for point 1 on chart = 406.

Average counts for point 4 on chart = 21896.

By comparison of the chart with the photograph of the same specimen, the point 2 on the chart is found to correspond to the point of density change on the photograph.

The composition of the alloy corresponding to point 2 is calculated as follows:

$$\text{Counts at the point} = (21896 - 406)\,\frac{47}{121} = 8347.$$

The ratio K_{zn} of intensity at the point to that of standard Zn is $\frac{8347}{74501}$, i.e., 0.1120.

The concentration of Zn is calculated by the use of the expression:

$$C_{zn} = K_{zn}\left[\frac{\alpha\ \text{spn.}}{\alpha\ \text{std.}}\right] \times \left[\frac{f(\lambda)\text{std.}}{f(\lambda)\text{spn.}}\right],$$

where the first factor is the atomic number correction factor and the second is the absorption correction factor.

No fluorescence correction is needed since Cu K lines lie on the long-wavelength side of the zinc absorption edge.

First iteration:

For evaluation of the correction factor, we assume that the $C_{zn} = 0.1120$ and $C_{cu} = 0.8880$.

α std. = α_{zn} = 7.2

α spn. = 7.2 x 0.1120 + 7.3 x 0.8880 = 7.2888

λ = $(\mu_1 M_1 + \mu_2 M_2)$ cosec 52.5°

λ std. = λ_{zn} = 49.3 x 1.2605 = 62.1427

λ spn. = (49.3 x 0.1120 + 42 x 0.8880) 1.2605 = 53.9719

$$\frac{1}{f(\lambda)} = 1 + a\left(\frac{\lambda}{\sigma_c}\right) + b\left(\frac{\lambda}{\sigma_c}\right)^2$$

For zinc, a = 1.08

b = 0.080

σ_c = 1780

$$\frac{1}{f(\lambda)_{std.}} = \frac{1}{f(\lambda)_{zn}} = 1 + 1.08\ \left(\frac{62.1427}{1780}\right) + 0.080\ \left(\frac{62.1427}{1780}\right)^2 = 1.0380$$

$$\frac{1}{f(\lambda)_{spn.}} = 1 + 1.08\ \left(\frac{53.9719}{1780}\right) + 0.080\ \left(\frac{53.9719}{1780}\right)^2 = 1.0328$$

Then, $C_{zn} = 0.1120 \times \frac{7.2888}{7.2000} \times \frac{1.0328}{1.0380} = 0.1128.$

The second iteration is done similarly, using the new value of C_{zn}.

Then, C_{zn} = 0.1128 once again.

Therefore the required concentration of Zn = 0.1128 or 11.28%.

Similarly the composition at the point 3 on the chart, which corresponds to the inner surface of the copper, is 23.52% Zn.

References:

1. Adler, Isidore. "X-Ray Emission Spectrography in Geology." Amsterdam, N.Y., Elsevier Pub. Co., 1966, pp. 201-217.

2. Cullity, B.D. "Elements of X-Ray Diffraction." Addison-Wesley Publishing Co., Inc., Reading, Mass., U.S.A., 1959, p. 466.

APPENDIX II

PROOF THAT DIFFUSIVITY "D" IS PROPORTIONAL TO x^2/t, WHERE "x" IS THE MEASURED PENETRATION DISTANCE AND "t" IS THE TIME OF DIFFUSION-ANNEAL

Let x_2 and x_1 be respectively the distances of a point on the final surface and another point corresponding to the concentration of the density change in the photograph with the original surface as origin (refer to Figure 10).

Balluffi and Seigle (55) have shown that the concentration C_2 at the solid-vapor interface remains constant throughout the diffusion run.

Then, assuming D to be independent of concentration,

$$C(x,t) = \tfrac{1}{2}\, C_o \operatorname{erfc} \frac{x}{2\sqrt{Dt}}$$

where C_o is the concentration at $x < 0$ at $t = 0$.

For test 1, with a time of diffusion-anneal "t_1,"

$$C_1(x_{11},t_1) = \tfrac{1}{2}C_o \operatorname{erfc} \frac{x_{11}}{2\sqrt{D_1 t_1}}$$

$$C_1(x_{21},t_1) = \tfrac{1}{2}C_o \operatorname{erfc} \frac{x_{21}}{2\sqrt{D_1 t_1}}$$

(The second subscript of "x" refers to the number of the test.)

From this it follows that,

$$C_1(x_{11},t_1) - C_1(x_{21},t_1) = \tfrac{1}{2}C_o\left[\operatorname{erfc}\frac{x_{11}}{2\sqrt{D_1t_1}} - \operatorname{erfc}\frac{x_{21}}{2\sqrt{D_1t_1}}\right]$$

$$= \tfrac{1}{2}C_o\left[\operatorname{erf}\frac{x_{21}}{2\sqrt{D_1t_1}} - \operatorname{erf}\frac{x_{11}}{2\sqrt{D_1t_1}}\right] \quad \ldots (1)$$

Similarly for test 2,

$$C_2(x_{12},t_2) - C_2(x_{22},t_2) = \tfrac{1}{2}C_o\left[\operatorname{erf}\frac{x_{22}}{2\,D_2t_2} - \operatorname{erf}\frac{x_{12}}{2\,D_2t_2}\right] \quad \ldots (2)$$

But $C_1(x_{11},t_1) = C_2(x_{12},t_2)$ ... (3)

and $C_1(x_{21},t_1) = C_2(x_{22},t_2)$ ... (4)

Then, from equations (1), (2), (3) and (4) it follows that,

$$\operatorname{erf}\frac{x_{21}}{2\sqrt{D_1t_1}} - \operatorname{erf}\frac{x_{11}}{2\sqrt{D_1t_1}} = \operatorname{erf}\frac{x_{22}}{2\sqrt{D_2t_2}} - \operatorname{erf}\frac{x_{12}}{2\sqrt{D_2t_2}}$$

i.e., $$\int_{\frac{x_{11}}{2\sqrt{D_1t_1}}}^{\frac{x_{21}}{2\sqrt{D_1t_1}}} e^{-n^2}\,dn = \int_{\frac{x_{12}}{2\sqrt{D_2t_2}}}^{\frac{x_{22}}{2\sqrt{D_2t_2}}} e^{-n^2}\,dn$$

Therefore, $$\frac{x_{21}}{2\sqrt{D_1t_1}} = \frac{x_{22}}{2\sqrt{D_2t_2}}$$

and $$\frac{x_{11}}{2\sqrt{D_1t_1}} = \frac{x_{12}}{2\sqrt{D_2t_2}}$$

Therefore, $$\frac{x_{21} - x_{11}}{2\sqrt{D_1 t_1}} = \frac{x_{22} - x_{12}}{2\sqrt{D_2 t_2}}$$

i.e., $$\frac{D_1}{D_2} = \frac{(x_{21} - x_{11})^2/t_1}{(x_{22} - x_{12})^2/t_2}$$

where $(x_{21} - x_{11})$ and $(x_{22} - x_{12})$ are the measured penetrations in the experiments.

References:

1. Crank, J. "The Mathematics of Diffusion." Clarendon Press, Oxford, 1956, pp. 11-13.

2. Balluffi, R.W. and Seigle, L.L. "Diffusion in Bimetal Vapor-Solid Couples." J. App. Phys., v. 25, no. 5, 1954, p. 607.

APPENDIX III

ANALYSIS OF CONDITIONS WHICH WOULD CAUSE ENHANCEMENT OF DIFFUSION BY PLASTIC DEFORMATION

Plastic deformation during diffusion may enhance diffusion by two possible mechanisms.

Enhancement of volume diffusivity by a vacancy mechanism is considered first. Strain generates vacancies in excess of those corresponding to thermal equilibrium. The mole fraction, N_v, of vacancies in thermal equilibrium at absolute temperature "T" is given by

$$N_v = \exp \frac{-Q_f}{kT} \exp \frac{S_f}{k} \qquad \ldots (1)$$

where Q_f and S_f are, respectively, the energy and entropy of formation of vacancies, and "k" is the Boltzmann's constant.

The excess number of vacancies, N_{xs}, produced by deformation would build up at a rate dependent on strain rate. In time dt, the increment of excess vacancies, would be

$$dN_{xs} = P\dot{\varepsilon}dt - \frac{N_{xs}dt}{\tau} \qquad \ldots (2)$$

which is the difference between the rate of generation and the rate of destruction, and where

P = atomic fraction of vacancies produced by unit strain,

$\dot{\varepsilon}$ = strain-rate, and

τ = life-time of a vacancy.

At steady state, $dN_{xs} = 0$.

Therefore $$P\varepsilon^{\bullet}\tau = N_{xs} \qquad \ldots (3)$$

Since D is proportional to the concentration of the vacancies,

$$\frac{D_s}{D_u} = \frac{N_v + N_{xs}}{N_v} \qquad \ldots (4)$$

where D_s = Diffusivity under strain, and

D_u = Diffusivity under static condition.

Substituting equation (3) in equation (4),

$$\frac{D_s}{D_u} = 1 + \frac{P\tau\varepsilon^{\bullet}}{N_v} \qquad \ldots (5)$$

"τ" is obtained from the number of jumps, "n," which a vacancy makes in time "t."

"n" is given by,

$$\frac{n}{t} = vz \exp\left(\frac{S_m}{k}\right) \exp\left(\frac{-E_m}{kT}\right) \qquad \ldots (6)$$

where v = mean atomic vibration frequency, and

z = co-ordination number, and

S_m and E_m are, respectively, the entropy and energy of vacancy movement.

In other words, the number of jumps per second is the product of the number of attempts per second, the number of possible jumps and the probability that the attempt will be successful.

Putting $$\frac{n}{t} = \frac{n_o}{\tau} ,$$

where n_o is the number of jumps which a vacancy makes before being captured, and eliminating v by the relation,

$$D_u = \frac{1}{12} a^2 z v N_v \exp(\frac{S_m}{k}) \exp(\frac{-E_m}{kT}) \quad \ldots (6a)$$

(a = lattice parameter)

one obtains:

$$\frac{D_s}{D_u} = 1 + \frac{Pa^2 n_o \varepsilon^\bullet}{12 D_u} \quad \ldots (7)$$

P is measured by resistometry at low temperatures.

$$P \simeq 10^{-3}.$$

Combining equations (6) and (6a), one obtains,

$$\frac{n_o}{\tau} = \frac{12\ D_u}{a^2 N_v}$$

Using the values of τ in the temperature region where it can be measured, and extrapolated values of D_u and N_v, one obtains $n_o \simeq 10^9$. This serves to identify the vacancy sinks as dislocations, since the mean distance travelled by a vacancy in its lifetime is $a\sqrt{n_o}$, which is nearly 10μ and this closely corresponds to the distance expected between dislocations in a well-annealed metal.

From equations (5) and (7),

$$\frac{P\tau}{N_v} = \frac{P n_o a^2}{12\ D_u}$$

The values are then obtained by extrapolation to the diffusion-temperature range from the annealing-temperature range.

Accuracy of a few percent in measuring D by conventional methods requires $\sqrt{Dt}$ be not less than 50μ. Since t cannot be more than a few weeks (10^6 sec.), values of D less than about 10^{-11} cm^2/sec. cannot be measured by conventional sectioning methods. For most metals a value of 10^{-11} cm^2/sec. for D corresponds to the temperature $(2/3)T_m$, where T_m is the absolute melting point. Thus for metals $(2/3)T_m$ is an estimate of the lower limit of the temperature to detect enhanced diffusion.

According to equation (5), a two-fold increase in D requires

$$\varepsilon^{\bullet} \simeq 10^{-2}/\text{sec.}$$

Such a strain rate is impractically high since the maximum total plastic strain that can be given to a metal is around unity and the corresponding time to reach it is too short for diffusion-anneal at temperatures lower than $(2/3)T_m$. But at temperatures high enough to measure D by conventional methods vacancies do not live long enough to affect the observed D.

Dislocation Diffusivity and Plastic Deformation: Suppose there are f dislocations per unit area and D' is the dislocation diffusivity. Then the fractional cross-section through which diffusion occurs by dislocations is fa^2, where a is the lattice parameter. For the remaining fraction diffusion occurs by volume diffusion with the diffusivity D.

Therefore the observed diffusivity is,

$$D_{obs.} = D\,(1 - fa^2) + D'fa^2$$

D' can be taken the same as for grainboundaries, since grainboundaries can be considered themselves as arrays of dislocations.

Hence $D' \simeq 10^6\, D$

$a^2 \simeq 10^{-15}\ cm^2$

Therefore $D_{obs.} \simeq D + D'fa^2$.

At $(2/3)T_m$, the metal is well annealed and remains so throughout.

Therefore, $f \gtrsim 10^8/cm^2$

Therefore, $D_{obs.} \gtrsim D\ (1 + \frac{1}{10})$, which is only just within the accuracy of measurement of D. However, at lower temperatures, it is possible to retain a higher concentration of dislocations such as $10^{11}/cm^2$ as in a fully work-hardened metal and large enhancements may be obtained.

References:

1. Brown, A.F. "The Effect of Vibrational Deformation on Diffusion-Controlled Reactions in Metals." App. Materials Research, v. 5, 1966, p. 67.

2. Lee, C.H., and Maddin, R. "The Effect of Torsional Strains on Self-Diffusion in Silver Single Crystals." Trans. AIME, v. 215, 1959, p. 397.

APPENDIX IV

EFFECT OF FATIGUE-CYCLING ON VOLUME DIFFUSION IN COPPER

Girifalco and Grimes show that,

$$\frac{D_s}{D_u} = 1 + \frac{N_{xs}}{N_v} \qquad \ldots (1)$$

where the symbols have the same significance as in Appendix III.

$$N_{xs} = \frac{K_1 \dot{\varepsilon}}{K_2} [1 - \exp(-K_2 t)] \qquad \ldots (2)$$

where K_2 is a parameter, giving the rate of vacancy loss, and

K_1 is a constant such that $K_1 \dot{\varepsilon}$ is the rate of vacancy production.

Thus $\frac{D_s}{D_u}$ can be computed if K_1 and K_2 are evaluated.

K_2 is a function of vacancy sinks. Considering only dislocations as effective vacancy sinks,

$$K_2 = \frac{2 D_v N_d}{\ln r/r_o} \qquad \ldots (3)$$

where D_v = diffusion coefficient of vacancies,

N_d = dislocation density,

$2r$ = distance between the sinks,

r_o = radius of a cylindrical dislocation sink.

Let us evaluate K_2 at 500°C under the conditions of the present experiments.

$D_v = 2 \times 10^{-8}$ cm^2/sec. (For analysis, see Appendix V.)

$N_d = 9 \times 10^8/\text{cm}^2$ (at room temperature)

(This is taken as the nearest representative data available.)

$r_o \simeq 10^{-8}$ cm.

$$r = \frac{1}{2 N_d} = \frac{10^{-4}}{6} \text{ cm.}$$

Therefore $$K_2 = \frac{2 \times 2 \times 10^{-8} \times 9 \times 10^8}{2.303 \log \frac{10^4}{6}}$$

$$= 4.8/\text{sec.}$$

$K_1 \simeq 10^{-3}$/sec.

t = Time to reach the strain-amplitude

$= 2 \times 10^{-2}$ sec.

$\dot{\varepsilon} = 3.82 \times 10^{-2}$/sec. (average value)

Substituting these values in the equation for N_{xs}, one obtains:

$N_{xs} = 0.73 \times 10^{-6}$

$$N_v \simeq \exp\left(\frac{-Q_f}{kT}\right)$$

where $Q_f \simeq 1$ ev/vacancy. (1 ev = 1.60×10^{-12} erg.)

Hence $$N_v = \exp\left(\frac{-1 \times 1.60 \times 10^{-12}}{1.38 \times 10^{-16} \times 773}\right).$$

$$= 3.16 \times 10^{-7}$$

Therefore, $$\frac{D_s}{D_u} = 1 + \frac{0.73 \times 10^{-6}}{3.16 \times 10^{-7}} \simeq 3.32.$$

Thus on the basis of this evaluation an enhancement by a factor of about 3.32 is expected. In the evaluation, the value of the dislocation-density, N_d, used is that at room temperature. But at 500°C, the actual value of N_d in the matrix would be less because fatigue damage is concentrated at grainboundaries and sub-cell walls. Therefore, if actual value were used, a still higher enhancement would be predicted.

No noticeable effect was observed on volume diffusion in the present experiments. This might be due to either of the following two reasons:

1. the number of excess vacancies generated within the volume of the grains during strain-cycling is too small to affect volume diffusion,
2. the vacancies generated by strain-cycling are too short-lived because of effective vacancy sinks.

But the second possibility is ruled out by the fact that in the matrix the concentration of dislocations is very low during fatigue damage, at higher temperatures. Therefore, it can be concluded that the number of excess vacancies generated by strain-cycling is too small to affect volume diffusion to any noticeable degree. Also any enhancement of diffusion can, therefore, occur only by "pipe diffusion" along dislocations in the cell walls.

A comparison of the value of the ratio D_s/D_u with equation (2) shows that the value of K_1 should be more than 2.32 times smaller than the used value (10^{-3}) for fatigue under the present conditions.

References:

1. Girifalco and Grimes, NACA Tech. Note 4408, 1958.

2. Riggs, B.A. "A Consideration of Diffusion in Strained Systems." Acta Met., v. 12, 1964, p. 952.

3. Grosskruetz, J.C., Reiman, W.H., and Wood, W.A. "Correlation of Optical and Electron-Optical Observations in Torsion Fatigue of Brass." Tech. Report No. 19, Inst. for the Study of Fatigue and Reliability, Columbia Univ., N.Y., 1964.

APPENDIX V

EVALUATION OF D_v, THE COEFFICIENT OF VACANCY DIFFUSION IN COPPER

$$D_v = D_o \exp\left(\frac{-E_m}{kT}\right) \quad \ldots (1)$$

where E_m = activation energy for migration of a vacancy, 1.19ev.

The average life-time of a vacancy is given by,

$$\tau = \frac{r_o^2}{\Pi^2 D_v} \quad \ldots (2)$$

where r_o = radius of spherical vacancy sink with a vacancy at the centre.

Combining equations (1) and (2), and taking logarithms,

$$\log \tau = \log r_o^2 - \log \Pi^2 - \log D_o + \frac{E_m}{2.3kT}$$

At $\frac{1}{T} = 0$, $\log D_o = \log r_o^2 - \log \Pi^2 - \log \tau$. $\ldots (3)$

The following table gives experimental data:

$10^4/T°K$	T°K	τ(sec.)	log τ
25.2	398	5340	3.728
23.6	423	690	2.839
22.3	448	112.8	2.052

From a plot of log τ vs. $10^4/T$ (see page 79),

$$\log D_o = \log r_o^2 - \log \Pi^2 - (-10.6)$$

Taking dislocations as sinks and the density of dislocations as $9 \times 10^8/cm^2$,

$$(2r_o)^2 = \frac{1}{9 \times 10^8} cm^2$$

Substituting for r_o,

$$\log D_o = +0.051.$$

At 500°C (773°K),

$$\log D_v = 0.051 - \frac{1.19 \times 1.6 \times 10^{-12}}{2.303 \times 1.38 \times 10^{-16} \times 773}$$

$$= \overline{8}.300, \quad \text{and}$$

$$D_v = 2 \times 10^{-8}$$

References:

1. Brinkman, J.A., Dixon, C.E., and Meechan, C.J. "Interstitial and Vacancy Migration in Cu_3Au and Cu." Acta Met., v. 2, 1954, p. 38.

2. Wood, et al. Tech. Report No. 19, Institute for Study of Fatigue and Reliability, Columbia University, New York, 1964.

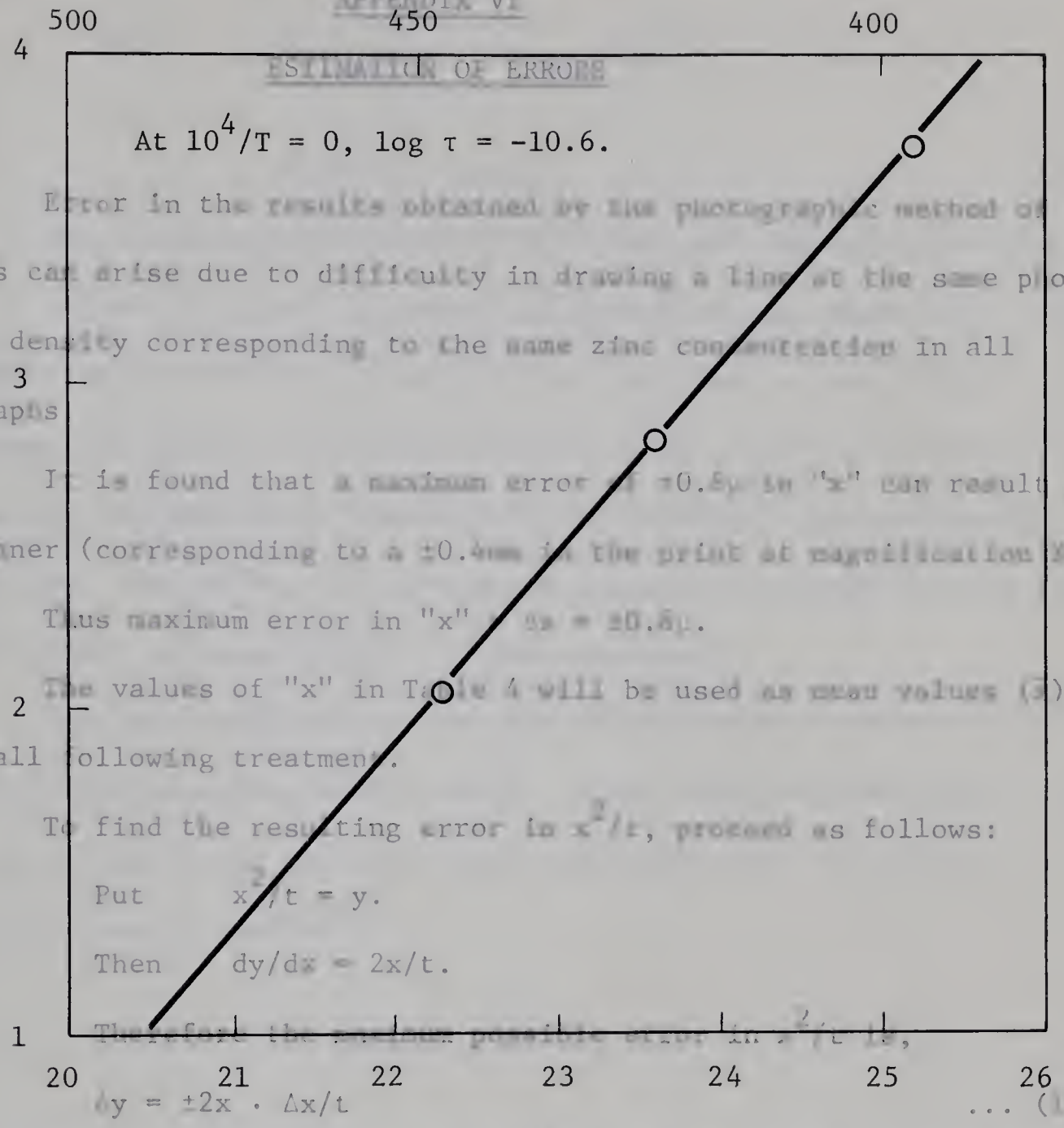

Figure 23. Plot of log τ versus $10^4/T°K$

Figure 23. Plot of log τ versus $10^4/T$°K

APPENDIX VI

ESTIMATION OF ERRORS

Error in the results obtained by the photographic method of analysis can arise due to difficulty in drawing a line at the same photographic density corresponding to the same zinc concentration in all photographs.

It is found that a maximum error of ±0.8μ in "x" can result in this manner (corresponding to a ±0.4mm in the print at magnification X487).

Thus maximum error in "x" = $\Delta x = \pm 0.8\mu$.

The values of "x" in Table 4 will be used as mean values ($\bar{x}$) of "x" in all following treatment.

To find the resulting error in x^2/t, proceed as follows:

Put $x^2/t = y$.

Then $dy/dx = 2x/t$.

Therefore the maximum possible error in x^2/t is,

$$\Delta y = \pm 2x \cdot \Delta x/t \qquad \ldots (1)$$

The corresponding values of x^2/t are tabulated in Table 7 for all observations. The maximum possible percentage errors in x^2/t values around the mean values are also provided in the same Table. It is seen that the percentage error decreases with an increase in the temperature of the experiment, if penetration distances are kept approximately the same for all tests. Observation of the errors in specimens 7S and 5S shows that the error is reduced by increasing the penetration distance.

To find the maximum possible error in the activation energy "Q", proceed as follows:

Put $z = \log(x^2/t)$.

Then $dz/dx = \frac{1}{x^2/t} \cdot 2x/t = 2/x$.

Therefore

$$\Delta z = \pm 2 \cdot \Delta x/x \qquad \ldots (2)$$

The corresponding values of x^2/t are also tabulated in Table 7.

A plot of $\log(x^2/t)$ versus $10^4/T$ is given in Figure 22. The calculated range of values of $\log(x^2/t)$ are plotted in this figure. From the diagram the maximum and minimum values of "Q" that may possibly be obtained by this method are found to be 45,300 and 33,500 cals/gmole respectively. Therefore, the activation energy as obtained by this method will be within the range 39,400 ± 5,900 cals/gmole.

However, it should be remarked that the above analysis was made to consider the maximum possible error. When lines are drawn they do not consistently follow the upper or lower boundaries and, therefore, the errors will be much smaller.

TABLE 7. Statistical Data

QUANTITY	SPECIMEN					
	6S	9S	8S	5S	4S	7S
Temperature	500° C	550° C	593° C	652° C	670° C	704° C
x^2/t	0.502±0.088	0.970±0.144	2.65±0.313	10.54±0.720	17.04±1.832	34.88±2.11
Percentage Error in x^2/t	±17.6	±14.8	±11.85	±6.84	±10.75	±6.05
$\log(x^2/t)$ range	$\bar{1}$.7007±0.174	$\bar{1}$.9868±0.1482	0.4233±0.1185	1.0228±0.0684	1.2315±0.1070	1.5426±0.0607
max. $\log(x^2/t)$	$\bar{1}$.8747	0.1350	0.5418	1.0912	1.3385	1.6033
min. $\log(x^2/t)$	$\bar{1}$.5267	$\bar{1}$.8386	0.3048	0.9544	1.1245	1.4819

TABLE 7 (continued).

QUANTITY	SPECIMEN					
	6D	9D	8D	5D	4D	7D
Temperature	500° C	550° C	593° C	595° C	630° C	704° C
x^2/t	0.588±0.094	1.02±0.1467	3.27±0.348	2.78±0.369	6 ± 1.08	36.29±2.15
Percentage Error in x^2/t	±16.0	±14.4	±10.6	±13.3	±18	±5.94
Log(x^2/t) range	$\bar{1}$.7694±0.1620	0.0086±0.1455	0.5146±0.1067	0.4400±0.1333	0.7782±0.1820	1.5598±0.00595
Maximum log(x^2/t)	$\bar{1}$.9314	0.1541	0.6213	0.5733	0.9602	1.6193
Minimum log(x^2/t)	$\bar{1}$.6074	$\bar{1}$.8631	0.4079	0.3067	0.5962	1.5003